THE ASTROPHYSICAL JOURNAL

AN INTERNATIONAL REVIEW OF SPECTROSCOPY AND ASTRONOMICAL PHYSICS

VOLUME 88 SEPTEMBER 1938 NUMBER 2

THE IMAGE-SLICER, A DEVICE FOR REDUCING LOSS OF LIGHT AT SLIT OF STELLAR SPECTROGRAPH

I. S. BOWEN

ABSTRACT

The fraction of the light in a stellar image that passes the slit of a spectrograph is calculated, and the limitations on any increase of this fraction by changes in the lens or mirror system are discussed.

It is shown that most of this light may be made to pass the slit by means of a device, here described, which slices up the image into a series of strips of a width equal to that of the slit and which arranges them end to end along the slit. The wide spectrum thus produced can be narrowed down by means of a cylindrical lens, thereby increasing the intensity of illumination at the photographic plate by factors ranging up to 10 or more.

The aberrations of the cylindrical lens used to narrow the spectrum are discussed.

I. EFFICIENCY OF A STELLAR SPECTROGRAPH IN THE USUAL ARRANGEMENT

The image of a star or other object, subtending an angle α, has a diameter

$$a = \alpha D_t F_t \tag{1}$$

at the focus of a telescope of aperture D_t and focal ratio F_t. If the spectrum of this stellar image is to be studied by a spectrograph whose collimator and camera lens have effective focal ratios F_c and F_s, the slit width must be

$$b = \frac{F_c \Delta}{F_s}, \tag{2}$$

in which Δ is the width of the slit image on the plate. If the full resolving-power of the spectrograph is to be attained, Δ must be made equal to, or less than, the resolving-power of the photographic plate, i.e., 20–40 μ. Assuming uniform illumination over a circular image, the fraction (R) of the light in the image passed by the slit is, then, approximately

$$R = \frac{4ab}{\pi a^2} = \frac{4F_c\Delta}{\pi F_s a D_t F_t}. \tag{3}$$

However, if all the light entering the spectrograph is to pass the collimator lens, it is necessary that $F_c \leq F_t$. The maximum efficiency of the slit therefore is

$$R = \frac{4\Delta}{\pi a D_t F_s}. \tag{4}$$

With the large-aperture telescopes that are now becoming available, combined with the spectrographs of large focal ratio, which the light-gathering power of these telescopes makes possible, the loss of light at the slit becomes very serious. Thus, in the case of the 200-inch telsecope, if $a = 1''$ (the approximate value for a star under good seeing conditions), $F_s = 30$, and $\Delta = 30\,\mu$, the efficiency will be only 5 per cent. For poor seeing conditions or larger nonstellar objects the fraction of light passed by the slit becomes even smaller.

From (4) it is evident that this efficiency R is independent of the focal ratio of the telescope or collimator lens. Thus, reducing the size of the stellar image, a, by changes from the Cassegrain to Newtonian arrangements or by the introduction of condensing lenses in front of the slit produces no change in the efficiency except for minor differences due to reflection or absorption losses in lenses or mirrors. This result may also be obtained in a more fundamental way from thermodynamic reasoning. Thus, one may show from the second law that it is impossible to decrease the area on which a given amount of radiant energy is concentrated without correspondingly increasing the size of the incident cone of light; i.e., as indicated in (1), the focal ratio of the incident light F_t must decrease proportion-

ately to the diameter of the image, a. Since, if the resolution is to be maintained, b must decrease proportionally to F_c and therefore to F_t, it is evident that the ratio of slit width b to image size a cannot be increased, and therefore the efficiency cannot be improved.

II. DESIGN OF IMAGE-SLICER

Since changes in area of the image are ineffective in increasing the efficiency, one is led to the remaining method of changing the shape of the image without altering its area. The optimum shape is obviously a long, narrow band whose width is equal to that of the slit.

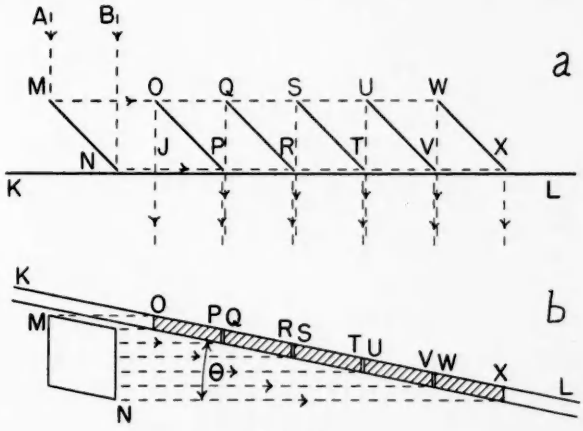

FIG. 1

If this can be accomplished by reflections at plane surfaces, the angle of the cone of incident light is not altered in any way, and therefore the equality of F_t and F_c is not disturbed.

This suggests the use of a system of plane mirrors which slice up the image into a series of strips which are then placed end to end along the slit. Two views of such a system of mirrors are shown in Figure 1, a and b. In this diagram the beam of light is assumed to come from a lens of large focal ratio and, consequently, to approximate a cylinder of uniform cross-section, equal to that of the image, in the immediate neighborhood of the focus. This beam, bounded by the rays AM and BN, is intercepted just before it reaches its focus by the 45° mirror MN, which is placed near one end and slightly to the side of the spectrograph slit KL (Fig. 1, b). This mirror is so

adjusted that the reflected beam bounded by the rays *MOQSUW* and *NPRTVX* is parallel to the plane of the slit jaws and just grazes their surface (Fig. 1, *a*). The mirror *MN* is rotated about the initial direction of the beam (*AM* or *BN*) into such a position that the reflected beam crosses over the slit *KL*, making a small angle θ with it (Fig. 1, *b*). A series of mirrors, *OP*, *QR*, *ST*, *UV*, and *WX*, whose widths are equal to that of the slit, *b*, are placed at intervals along the slit where the reflected beam crosses it. They are made parallel to the first mirror, *MN*, and are therefore inclined at 45° to the beam. As the reflected beam passes over the slit, each of these mirrors intercepts a strip equal in width to the slit and reflects it downward through the slit in a direction parallel to the original beam.

The mirrors placed over the slit have the same width as the slit (0.02–0.5 mm) and a length of 0.5–2.0 mm. It is, therefore, not feasible to make and accurately mount mirrors of just this size. Fortunately, the light does not pass over the slit, and consequently the mirrors may be parts of surfaces that extend as far as is convenient in the direction above the slit in Figure 1, *b*.

Figure 2 indicates a design for mounting these mirrors, of which the parts that are used (i.e., that correspond to mirrors *OP*, *QR*, *ST*, *UV*, and *WX* in Fig. 1) are indicated by the shaded areas. The reflecting surfaces are evaporated aluminum films applied to glass plates whose thicknesses are equal to the perpendicular distances between the mirrors of Figure 1. The reflecting surfaces may therefore be properly spaced by stacking the glass plates in contact with each other. These plates must be shaped and mounted in such a way as to satisfy the following conditions. (1) The separate slices of the image, *JP*, *PR*, *RT*, *TV*, and *VX*, should have a length equal to the diameter *a* of the star image, and a width equal to that of the slit *b*. (2) The successive slices should be laid down end to end on the slit with the sides of successive sections forming one continuous line, i.e., without jogs or spaces between adjacent slices. (3) The direction of the beams entering the slit should be parallel to the initial beam *AM*, *BN*. (4) No parts of the glass plates except the aluminized areas should interfere with either the incident or reflected beams.

From the foregoing conditions the following details of design can be deduced at once.

1. The thickness T of the plates should equal $a/\sqrt{2}$, in which a is the diameter of the star image.

2. The number of plates should be equal to a/b in which b is the slit width.

3. As has been already stated, the plane DPE of the mirror should make an angle of 45° with the plane EPK of the slit jaws.

4. $\angle KPE$, i.e., the angle between the slit KP and the intersection of the plane of the mirror with the plane of the slit jaws, should be $\pi/2 - \theta$, in which $\theta = \sin^{-1} b/\sqrt{2}\,T = \sin^{-1} b/a$. As noted above, θ is also the angle at which the first reflected beam crosses the slit.

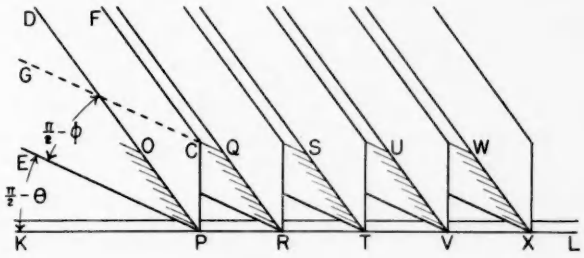

FIG. 2

5. The angle between the surface of the mirror DPE and the surface CPE should be 45° or less.

6. $\angle DPE$ should equal $\pi/2 - \phi$, in which $\tan \phi = (\tan \theta)/\sqrt{2}$.

7. The angle between the plane of the mirror DPE and the plane CPD should be $\pi/2 - \phi$ or less.

8. The plane of the mirror MN should be parallel to plane DPE.

9. The focus of the telescope should be adjusted to come at the point in the first reflected beam $MOQRST$, where it strikes the center one of the small mirrors.

If the cones of light reflected by the small mirrors OP, QR, etc., are exactly parallel, they fail to coincide at the collimator lens by an amount equal to the distances between these mirrors. In case the distance between the end mirrors becomes an appreciable fraction of the diameter of the collimator lens, this may result in a significant

loss of light. However, by making the mirror plates slightly wedge-shaped, with an angle $a/2f_c$ (a = image size, f_c = focal length of collimator) between the faces EPD and GCF, the mirrors are given the correct tilt to bring the cones into coincidence at the collimator lens. In this case the center mirror, only, makes an angle of exactly 45° with the plane of the slit jaws.

The mirror MN is obviously not an essential part of the image-slicer and may be eliminated in cases where it is feasible to mount the spectrograph with its axis at right angles to that of the telescope.

By following the foregoing procedure it is possible to make practically all the light in the image pass the slit, except for the necessary loss at the two (or one) reflections; i.e., the efficiency of this system can be brought up to from 75 to 90 per cent, as compared with the 5 per cent obtained in the example cited above. The foregoing process, however, operates by lengthening the section of the slit that is illuminated rather than by increasing the amount of light passing the unit length of the slit. The image-slicer by itself does not, therefore, increase the intensity of illumination on the photographic plate, but instead gives a much wider spectrum. Thus, in the example of the 200-inch telescope cited above, the spectrum will have a width of $\frac{3}{4}$ mm as normally used and of 18 mm when the image-slicer is introduced.

Since the width of the spectrum obtained with the image-slicer is usually much greater than is necessary, it becomes advisable to narrow the spectrum down with a cylindrical lens and thereby obtain the corresponding increase in the intensity of illumination on the plate. The next two sections contain a brief discussion of the use of the cylindrical lenses and the limitations imposed by the aberrations inherent in them.

III. USE OF CYLINDRICAL LENS TO DECREASE WIDTH OF SPECTRUM

As normally used, the cylindrical lens is placed in front of the plate with the axis of its cylindrical surface parallel with the dispersion of the spectrum. In this position the focal plane of the spectral lines is only very slightly changed by its presence. The position of the cylindrical lens is adjusted so that the photographic plate and the exit pupil of the spectrograph (either grating, prism, or camera

lens) are at conjugate foci of the cylindrical lens. Since the width, W, of the spectrum desired is almost always very small compared with the diameter of the exit pupil, the focal length of the cylindrical lens is small compared with that of the spectrograph camera, and the distance between plate and cylindrical lens is very nearly equal to the focal length of this lens. The focal length of the cylindrical lens is made equal to the width, W, of the spectrum desired, times the focal ratio F_s of the spectrograph camera lens. The width of the cylindrical lens should be slightly greater than the width of the spectrum formed before its introduction. Since it is often desirable to reduce the width of the spectrum by a factor of from 10 to 20, cylindrical lenses of low focal ratio are required. It is, therefore, necessary to investigate the aberrations introduced by their presence.

IV. EFFECT ON DEFINITION OF SPECTRAL LINES OF ABERRATIONS INTRODUCED BY CYLINDRICAL LENS

The calculation of the aberrations of a cylindrical lens depends on the following easily proved theorem.[1] *If any plane be drawn through the normal to a surface between two media, the sine of the angle between this plane and any ray drawn through the foot of the normal is to the sine of the angle between this plane and the refracted ray inversely as the ratio of the indices of the two media.*

Through the cylindrical lens $ABCD$ in Figure 3 pass a plane EF normal to the axis of the cylinder and therefore cutting all surfaces of the cylindrical lens normally. The plane EF therefore intersects the photographic plate KL in a line parallel to the spectral lines. Allow any ray $GHIE$ to pass through the lens. Since the plane EF is normal to all surfaces, the sine of the angle between the ray and the plane EF must at all points be inversely proportional to n, the index. Therefore, the total distance d that the ray approaches the plane EF is

$$d = \sin \beta \sum \frac{l}{n}, \tag{5}$$

in which β is the angle between the ray and the plane EF in air and l is the distance along the ray.

[1] J. P. C. Southall, *Principles and Methods of Geometrical Optics*, p. 30, New York: Macmillan Co., 1910.

Consider two rays coming from the same point on the grating and making the same angle β with the plane EF in air. One of these rays passes through the center of the cylindrical lens, the other through the edge. The geometrical path from grating to plate, $\sum l$, through the center of the lens is shorter than that through the edge of the lens by an amount D.

If the surfaces of the cylindrical lenses are aplanatic surfaces, the optical length $\sum nl$ of the two paths must be equal. In order to satisfy this condition, it is necessary that the central ray pass through $D/(n-1)$ greater thickness of glass than the outer one and that

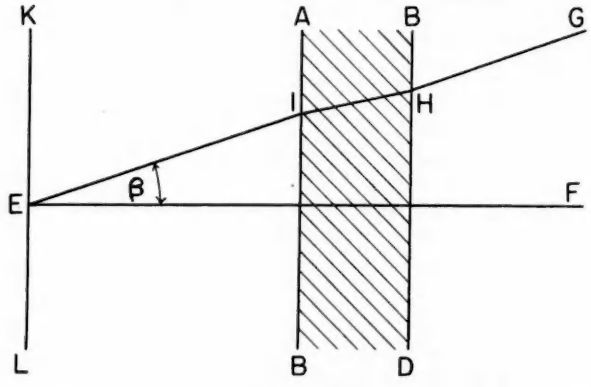

FIG. 3

the ray through the edge pass through $nD/(n-1)$ greater thickness of air than the central one. In passing through $D/(n-1)$ of glass the central ray approaches the plane EF by the distance (sin β) $D/n(n-1)$, while the edge ray in passing through $nD/(n-1)$ of air approaches it by the distance (sin β) $nD/(n-1)$. At the focus these rays are therefore separated by a distance sin $\beta\,[nD/(n-1) - D/n(n-1)] = (\sin\beta)\,D(n+1)/n$ in the direction normal to EF, i.e., normal to the spectral line.

If the photographic plate, and therefore the axis of the cylindrical surface of the lens, is normal to the axis of the cone of incident light, the maximum value of sin β is $\frac{1}{2}F_s$, which means that the width of the spectral lines, δ, due to this aberration is

$$\delta = \frac{D(n+1)}{2F_s n}. \tag{6}$$

Case 1. Single thin cylindrical lens.—The difference in geometrical path between the central and edge rays of a single thin cylindrical lens of focal ratio F_K and of focal length WF_s is

$$D = \frac{WF_s}{8F_K^2}$$

and

$$\delta = \frac{(n+1)W}{16nF_K^2}. \tag{7}$$

The minimum value of F_K that may be used, if no aberrations greater than δ are permissible, is for normal incidence

$$F_K = \frac{1}{4}\sqrt{\frac{(n+1)W}{n\delta}}. \tag{8}$$

For $n = 1.5$, $W = 1$ mm, and $\delta = 25\,\mu$ this gives $F_K = 2.04$. This represents about the minimum value of F_K that can be obtained with a single cylindrical lens. If the lens surfaces are circular cylinders, approximately the same limit is set by the aberrations, parallel to the spectral lines, becoming an appreciable fraction of W at $F_K = 2$.

Case 2:—Aberrations of a system of cylindrical lenses.—From the foregoing discussion it is evident that the aberration across the spectral line is proportional to the difference in geometrical path of the rays through the center and edge of the cylindrical lens. Qualitatively, it is at once evident that the path difference can be cut down by dividing the refraction between two lenses. Thus, in Figure 4, if the refraction takes place at a single thin lens BB', we have the path ABF for the extreme ray. On the other hand, if the refraction is split between the two lenses EE' and GG', the edge path becomes $AEGF$. This, obviously, is shorter and consequently differs less from the central ray CF, although the focal ratio $F_K = \frac{1}{2}\sin \angle CFB$ remains the same.

Quantitatively, it can easily be shown that the difference in path D between the central or axial ray and the edge ray, which are as-

sumed to be originally parallel, is $\sum m \tan \gamma/2$, where m is the distance to which the edge ray approaches the axis and γ is the angle between the edge ray and the central undeviated ray. Since $\sum m$ is the distance between the rays before the first lens is reached, it is evidently important to keep γ as small as possible at all points.

For a spectrum of finite width it is impossible to decrease D indefinitely by making FG' approach zero and $G'E'$ become very large since the width of the cone of light from EE', which increases with $G'E'$, becomes greater than the width of the lens GG', which must decrease with FG'. However, by making the lens GG' a very thick

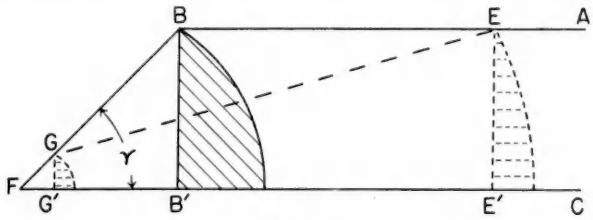

FIG. 4

plano-convex lens whose plane face is placed in contact with the photographic plate, is it possible to almost completely eliminate the path, where γ has its maximum value of $\sin^{-1} \frac{1}{2} F_K$, over as wide a spectrum as may be desired. If, following this design, the lens GG' has a radius of curvature r and a thickness $(1 + e)r$, and the lens EE' is a thin lens of focal length $nWF_s/(e + 1 - ne)$, the minimum value of F_K that may be used without the spectral line width exceeding δ is

$$F_K = \frac{1}{4n} \sqrt{\frac{n+1}{\delta}\left[\frac{(e+1)er(n-1)}{F_s n} + W(e+1-ne)\right]}. \quad (9)$$

These yield the results shown in Table 1.

Since the width of the lens GG' must be large compared with the width of the spectrum formed by EE', it is evident that r must be of the order of 5 mm or more if $W = 1$ mm. The last two rows of Table 1 give the numerical values of F_K for $W = 1$ mm, $r = 5$ mm, $\delta = 25\ \mu$, and $F_s = 30$ and for the values of n indicated. The case $e = 1/n$ eliminates all aberrations along the spectral lines due to

lens GG', and those introduced by EE' are small. Case $e = 1$ is closely approximated by the use of a complete circular rod for lens GG'.

If the axis of the cone of incident light is not normal to the axis of the cylindrical surface of the lens, but makes an angle θ with the normal plane, the maximum value of sin β is approximately sin $\theta + (\cos \theta)/2F_s$. In this case the value of the aberration δ in equations (6) and (7) is multiplied by the factor $(2F_s \sin \theta + \cos \theta)$.

TABLE 1

e....	0	$1/n$	1
F_K	$\frac{1}{4n}\sqrt{\frac{(n+1)W}{\delta}}$	$\frac{1}{4n}\sqrt{\frac{n+1}{\delta}\left[\frac{(n^2-1)r}{F_s n^3}+\frac{W}{n}\right]}$	$\frac{1}{4n}\sqrt{\frac{n+1}{\delta}\left[\frac{2(n-1)r}{F_s n}+W(2-n\right]}$
Focal length of lens EE'.....	$WF_s n$	$WF_s n^2$	$\frac{WF_s n}{2-n}$
Width of spectrum formed by EE' alone.....	Wn	Wn^2	$\frac{Wn}{2-n}$
$F_K(n = 3/2)$.....	1.67	1.42	1.30
$F_K(n = 5/3)$.....	1.55	1.26	1.06

Likewise, the lowest permissible value of the focal ratio F_K for a given δ is increased by the factor of $\sqrt{2F_s \sin \theta + \cos \theta}$ in equations (8) and (9) and in Table 1.

V. METHODS FOR GUIDING TELESCOPE

Since none of the light strikes the slit jaws when the image-slicer is in place, a change in the usual method of guiding the telescope is required. One procedure is to replace the first mirror MN by a right-angle prism to the first surface of which has been cemented, with Canada balsam, a thin wedge of glass with an angle of 2°–5° between its faces. The upper surface of the wedge is aluminized except for an area equal to the cross-section of the incident beam, which at that point is only slightly larger than the image diameter a. Owing to the angle between the incident beam and the normal to the upper surface of the wedge, any light reflected by this surface can be observed

by a microscope placed at an appropriate position beside the incident beam. As long as the telescope is properly pointed, only 4–5 per cent of the light is reflected at the glass air surface of the unaluminized section. If the telescope drifts from its correct direction, part of the image moves over on the aluminized area and a large fraction of the light is reflected. Because of the slight refraction of the main beam AM, BN, in passing through the wedge, a small tilt must be given to right-angle prism to bring the initial and final beams into parallelism.[2]

ASTROPHYSICAL OBSERVATORY
CALIFORNIA INSTITUTE OF TECHNOLOGY
June 1938

[2] A second article will give the results of performance tests, details of mounting the mirrors, and methods of construction of the optical parts.

FRAUNHOFER INTENSITIES IN THE INFRARED REGION λλ 8800–11830 A*

C. W. ALLEN[1]

ABSTRACT

Equivalent breadths, measured photometrically on spectra taken with an 18-foot focus spectrograph at Mount Wilson Observatory, are tabulated for 188 absorption lines in the solar spectra between λ 8800 and λ 11830 A.

Systematic observations of the intensities of Fraunhofer lines have already been published by the author for the visual[2] and the near infrared spectrum.[3] Since for many solar problems it is desirable that such information should cover as wide a wave-length range as possible, the observations have been extended as far into the infrared as the available plates would allow.

Photometry.—Spectra of the center of the sun's disk were obtained with an 8-inch Michelson plane grating mounted at the 18-foot focus of the spectrograph pit of the Snow telescope of the Mount Wilson Observatory. The plates were Eastman 144P, 144M, 144Q, 1Z, backed and ammoniated, and developed for 5 minutes at 65° F with a hydroquinone developer of strong contrast (X-ray). Usually three spectra of varying exposure times were recorded on each plate, the best two being selected for photometry. The plates were standardized with solar spectra taken through a step-slit and with similar exposure times. For this purpose the intensity of the sun's image was decreased by inserting a number of black cheesecloth screens into the telescope beam. For each measurable line the uncorrected central intensity, r_m, and the measured breadth of the line at half its maximum depth, Δ_m, were obtained. For the majority of lines the equivalent breadth is then given by $W = 1.22\,\Delta_m(1 - r_m)$, where the numerical factor is obtained from considerations of scattered

* *Contributions from the Mount Wilson Observatory, Carnegie Institution of Washington*, No. 594

[1] Hackett Research Student.

[2] *Mem. Commonwealth Solar Obs. Canberra*, **1**, No. 5, 1934.

[3] *M.N.*, **96**, 843, 1936.

light and line contour. For the strongest lines the factor is somewhat greater. This procedure enables allowance to be made for the appreciable difference in the breadth of Fraunhofer lines in the infrared. The effect of this difference was not realized when my last intensity list[3] was published, and hence the equivalent breadths of a few of the broadest lines given in that list may be too small.

An attempt has been made to correct r_m for the blending of atmospheric or solar lines. When it was not possible to measure Δ_m, a mean value for the region was adopted.

With the exception of a few gaps, four plates covered each region from λ 8800 to λ 11000 A. Beyond 11000 A, however, only one badly fogged plate was available, and the results must be regarded as tentative. Where different type of plates overlapped, there was some evidence that plates of higher contrast gave systematically smaller equivalent breadths. It is hoped to investigate this question later, but for the present the mean is taken. The present observations are in reasonable agreement with those of Minnaert and Bannier.[4] The comparison was made, however, in a region where there is no blending with atmospheric lines, and hence the agreement may give an exaggerated impression of the general accuracy.

Results.—The results are given in Table 1. The first four columns contain material kindly supplied to me in advance of publication by Mr. H. D. Babcock and Dr. Charlotte E. Moore. Some of the wave lengths, especially beyond 11000 A, may be further improved by small changes. The intensities, by Miss Moore, are not in every case final. They are designed to be concordant with Rowland's intensities in the region near λ 6200. The fifth column contains the equivalent breadths, W, resulting from the present investigation; the sixth, the corresponding results of Minnaert and Bannier[4] (MB), Dahme[5] (Da), and Minnaert and Genard[6] (MG). All values are in milliangstroms. The last column gives the quantity W/λ, which is often more convenient in application than W itself.[7] These values of W are averages from the two preceding columns. More doubtful values of W are in parentheses.

[4] *Zs. f. Ap.*, **11**, 392, 1936.

[5] *Ibid.*, **11**, 93, 1935.

[6] *Ibid.*, **10**, 377, 1935.

[7] D. H. Menzel, *Ap. J.*, **84**, 462, 1936.

TABLE 1

Wave Length	Element	E.P.	Intensity	W in Milliangstroms		$10^6 W/\lambda$
				Author	Others	
					MG	
8804.637	*Fe*	2.269	3	56	.....	6.4
8806.775	*Mg*	4.327	12	495	512	57.2
8808.173	*Fe*	.....	1	35	.....	4.0
8809.406	*Ni*	3.881	−2	32	.....	3.6
8824.236	*Fe*	2.188	9	181	.....	20.5
8838.441	*Fe*	2.846	6	102	.....	11.6
8846.750	*Fe*	.....	3	52	.....	5.9
8862.054	⊙	.....	−2	20	.....	2.3
8862.563	*Ni*	4.072	3	61	.....	6.9
8866.943	*Fe*	4.529	8	154	.....	17.4
8868.443	*Fe*⁻	.....	3	50	.....	5.7
8876.031	*Fe*	.....	1	34	.....	3.8
8883.68	*Si*	5.928	−2	13	.....	1.5
8884.24	*S*	.....	−3	10	.....	1.1
8892.738	*Si*	5.958	4	77	.....	8.7
8899.222	Atm?	.....	2	46	.....	5.2
8905.989	⊙	.....	0	23	.....	2.6
8912.101	⊙	.....	7	113	.....	12.7
8920.036	*Fe*, Atm? (*V*)*	5.042	3	61	.....	6.8
8923.570	*Al*	.....	3	61	.....	6.8
8924.69	⊙	.....	−2	33	.....	3.7
8927.392	⊙	.....	4	123	.....	13.7
8943.058	*Fe* (*Na*??)*	.....	1	49	.....	5.5
8945.198	*Fe*	5.011	3	80	.....	8.9
8947.197	*Cr*	.....	−2	(17)	.....	1.9
8950.217	*Fe*	.....	−3	10	.....	1.1
8967.72	⊙?	.....	−2	(18)	.....	2.0
8968.20	*Ni*	.....	−2	24	.....	2.7
8975.413	*Fe*	2.977	−1	81	.....	9.0
8976.88	*Cr*	.....	−2	18	.....	2.0
8979.23	⊙?	.....	−3	18	.....	2.0
8984.898	*Fe*	5.078	−1	32	.....	3.6
8999.580	*Fe*	2.819	2	126	.....	14.0
9008.52	*Fe*?	.....	0	68	.....	7.6
9009.835	*Cr*	3.307	0	62	.....	6.9
9010.573	*Fe*	.....	0	33	.....	3.7
9013.98	*Fe*	.....	−1	22	.....	2.4
9019.77	*Fe*	5.078	−2	21	.....	2.3
9021.57	*Cr*	3.309	1	58	.....	6.4
9024.38	*Fe*	.....	0	(62)	.....	6.9

* Parentheses indicate masked.

TABLE 1—*Continued*

Wave Length	Element	E.P.	Intensity	*W* in Milliangstroms		$10^6 W/\lambda$
				Author	Others	
9030.75	*Fe*	.....	− 2	21	... .	2.3
9035.88	*Cr*	.....	− 3	16	... .	1.8
9051.47	⊙?	.....	− 2	(28)	... .	3.1
9061.443	*C*	7.450	1	(126)	... .	14.0
9070.416	*Fe*	.....	− 2	32	... .	3.5
9078.28	*C*	7.450	1d?	116	... .	12.8
9088.391	*Fe, C*	.....	2d?	207	... .	22.9
9089.422	*Fe*	.....	1	(90)	... .	9.9
9094.898	*C*	7.455	3N	226	... .	24.8
9103.67	*Fe*? Atm?	4.160	− 1	21	... .	2.3
9111.877	*C*	7.455	2	155	... .	17.0
9116.26	*Fe*	.....	− 2	24	... .	2.6
9146.16	Atm (*Fe*)*	2.557	1	52	... .	5.7
9210.036	*Fe*	2.833	1	64	... .	6.9
9218.251	⊙	.....	0	63	... .	6.8
9228.101	*S*	6.496	1	104	... .	11.3
9237.56	*S*	6.496	0	95	... .	10.3
9248.76	⊙	.....	− 3	22	... .	2.4
9253.71	Atm? *Fe*?	.....	0	48	... .	5.2
9255.79	⊙	.....	3	202	... .	21.8
9258.280	*Fe*	4.588	1N	87	... .	9.4
9263.93	*Cr*	.....	− 2	29	... .	3.1
9290.468	*Cr*	2.532	− 2	46	... .	4.9
9405.27	*C*?	.....	− 1N	(177)	... .	18.8
9414.95	*Mg*	.....	2N	(202)	... .	21.5
9432.73	⊙?	.....	0	(88)	... .	9.3
9434.82	Atm	.....	0N	(30)	... .	3.2
9447.03	*Cr*	2.534	− 1	(63)	... .	6.7
9462.94	*Fe*	.....	− 1N	(43)	... .	4.6
9574.29	*Cr*, Atm?	2.534	0N	(62)	... .	6.5
9603.231	*C*	7.450	1N	(79)	... .	8.2
9638.39	*Ti*	.....	2	(116)	... .	12.0
9647.34	*Ti*	.....	− 3	28	... .	2.9
9658.40	*C*	7.455	0N	151	... .	15.6
9675.571	*Ti*	.....	0	74	... .	7.6
9689.37	*Si*	.....	− 1	(55)	... .	5.7
9699.58 9699.76	Atm, *Fe*	.....	− 3N	(39)	... .	4.0
9705.366 9705.679	Atm *Ti*	.....	0 0	(73)	... .	7.5
9726.27	⊙?	.....	− 3	(17)	... .	1.7
9728.55	*Ti*	.....	− 1N	(67)	... .	6.9

TABLE 1—*Continued*

Wave Length	Element	E.P.	Intensity	*W* in Milliangstroms		$10^6 W/\lambda$
				Author	Others	
					MB Da	
9753.10	*Fe*, Atm	4.775	− 2	(72)	... .	7.4
9764.13	⊙? Atm?	.....	− 1N	(66)	... .	6.8
9800.29	*Fe*	.....	− 1N	(62)	... .	6.3
9834.12, 9834.22	*Fe*	.....	− 3N	32	... .	3.3
9839.36	*Si*, *Fe*	.....	− 3	22	... .	2.2
9854.66	⊙? Atm?	.....	− 3N	29	... .	2.9
9861.746	*Fe*	.....	1	80	... .	8.1
9868.12	*Fe*	.....	0N	72	... .	7.3
9887.05	*Si*?	.....	1	28	... .	2.8
9889.052	*Fe*	.....	5	82	... .	8.3
9890.67	⊙	.....	3N	69	... .	7.0
9891.61	−*Si*	.....	2d?	28	... .	2.8
9913.19	*Si*, *Fe*	.....	2	34	... .	3.4
9930.49	⊙	.....	0N	20	... .	2.0
9931.45	⊙	.....	3N	51	... .	5.1
9944.220	*Fe*	.....	3	32	... .	3.2
9980.48	*Fe*	.....	2	24	... .	2.4
9986.490	⊙	.....	3	35	... .	3.5
9993.17	*Mg*	.....	3	68	... .	6.8
9994.94	⊙	.....	2	29	... .	2.9
9997.665	⊙	.....	2	34	... .	3.4
10036.670	Sr^+	1.797	5	78	88	8.3
10048.64, 10049.27	*H*	12.04	5N, 50NN	1390	... 1810	160.0
10057.68	*Ti*, *Fe*	.....	2	28	18	2.3
10065.070	*Fe*	4.814	8	100	77	8.9
10068.39	⊙	.....	2	27	... .	2.7
10123.895	⊙	.....	8	88	103	9.4
10145.580	(*Ni*),* *Fe*	.....	10	132	143	13.6
10193.245	*Ni*	.....	4	51	... .	5.0
10195.12	*Fe*	2.716	2	22	... .	2.2
10216.335	*Fe*	4.713	9	128	134	12.8
10218.415	*Fe*	.....	3	43	... .	4.2
10288.950	*Si*	4.899	6	94	81	8.5
10302.62	*Ni*	.....	2	37	... .	3.6
10327.360	Sr^+	1.832	7	147	139	13.9
10330.22	*Ni*	.....	2	31	... .	3.0
10340.900	*Fe*	2.188	3	51	43	4.5
10343.840	*Ca*	2.920	8	143	141	13.7
10347.975	*Fe*	.....	3	39	28	3.2
10353.82	*Fe*	.....	2	26	17	2.0

TABLE 1—*Continued*

Wave Length	Element	E.P.	Intensity	*W* in Milliangstroms		$10^6 W/\lambda$
				Author	Others	
					MB	
10371.285	*Si*	4.908	9	173	177	16.9
10378.620	*Ni*	.....	3	76	63	6.7
10395.795	*Fe*	2.167	4	61	61	5.9
10396.81	*Ti*	.....	2	34	36	3.4
10452.74	*Fe*	.....	3	44	54	4.7
10455.450	*S*	.....	7	113	130	11.6
10456.74	*S*	.....	4	67	61	6.1
10459.430	*S*	.....	7	102	107	9.9
10469.680	*Fe*	.....	7	91	91	8.7
10486.30	*Cr*	.....	3	(22)	25	2.3
10496.16	*Ti*	.....	3	(18)	...	1.7
10530.55	*Ni*	.....	2	(25)	17	1.9
10532.24	*Fe*	.....	4	62	54	5.5
10535.70	⊙	.....	2N	(38)	...	3.6
10582.17	*Si*⁻	6.196	2	(29)	...	2.7
10585.165	*Si*	4.932	12	350	...	33.1
10603.440	*Si*	4.908	10	249	...	23.5
10627.63	*Si*	.....	8	136	...	12.8
10660.98	*Si*	4.899	10	275	...	25.8
10683.11	*C*	7.450	9	205	...	18.5
10685.35	*C*	7.452	8	164	...	15.4
10689.73	*Si*	5.928	8	186	...	17.4
10691.25	*C*	7.455	9	255	...	23.9
10694.23	*Si*	5.938	8	189	...	17.7
10707.32	*C*	7.452	8	145	...	13.5
10727.41	*Si*	5.958	9	231	...	21.6
10729.47	*C*	7.455	7	177	...	16.5
10749.37	*Si*	4.908	12	284	...	26.5
10753.98	*C*	.....	0	(55)	...	5.1
10783.05	*Fe*	.....	1	46	...	4.3
10784.58	*Si*	5.938	3	98	...	9.1
10786.85	*Si* (*Al*)*	.....	7	246	...	22.9
10818.31	*Fe*	.....	1	(49)	...	4.5
10827.14	*Si*	4.932	12	430	...	39.7
10830.31	*He*??	19.74	− 2N	(26)	...	2.4
10834.01	*Na*??	.....	5	106	...	9.8
10843.89	*Si*	6.159	5	212	...	19.6
10863.50	*Fe, Ca*	.....	3	100	...	9.2
10869.57	*Si*	.....	4	580	...	53.3
10882.84	*Si*	.....	3	108	...	9.9

TABLE 1—*Continued*

Wave Length	Element	E.P.	Intensity	*W* in Milliangstroms		$10^6 W/\lambda$
				Author	Others	
					Da	
10885.37	*Si*	6.154	3	145	.....	13.3
10896.34	*Fe*	.....	2	41	.....	3.8
10905.74	*Fe? Cr*	.....	1	36	.....	3.3
10914.26	*Fe?*$^-$	.....	2	44	.....	4.0
10914.90	*Sr*$^+$	.....	5	155	.....	14.2
10937.26 10938.07 10938.68	*H*	12.04	50NN 2NN	1320	2190	160.0
10962.30	*Mg?*	5.906	3N	46	.....	4.2
10965.45	*Mg?*	5.907	5N	210	.....	19.2
10979.34	*Si*$^-$, *Ni*	.....	4	307	.....	28.0
10982.11 10982.39	*Si*	6.164	2 4	228	.....	20.8
10984.42	*Si*	6.164	3	151	.....	13.8
11018.23	*Si*$^-$	.....	10	577	.....	52.4
11198.57	*Ni*	.....	4	(215)	.....	19.2
11371.98	*Fe*$^+$	.....	3N	(220)	.....	19.4
11403.86	−*Na*	2.095	1N	(195)	.....	17.1
11422.38	*Fe*	.....	1	(107)	.....	9.4
11592.24	*Si*	.....	0	177	.....	15.3
11660.69	*C??*	.....	8N	888	.....	76.5
11604.51	*C??*	.....	0	287	.....	24.7
11607.67	*Fe*	2.188	− 1	155	.....	13.3
11611.65	*Si*	.....	1N	410	.....	35.3
11638.27	*Fe*	2.167	0?	175	.....	15.1
11690.38	*K*	.....	0	(318)	.....	27.2
11750.03	*C?*	.....	8	(180)	.....	15.3
11751.23	*C?*	.....	− 1	(253)	.....	21.5
11754.85	*C?*	.....	0	(325)	.....	27.7
11772.75	−*K*	.....	1N	(305)	.....	26.0
11828.39	*Mg*	4.327	0	(440)	.....	37.1

A study of intensities within multiplets and groups of multiplets is being made from the infrared equivalent breadths now available. For a complete understanding of such problems, however, it is very desirable that intensity observations in the λλ 3000–4000 A region of the solar spectrum should be made, and it is to be hoped that an observatory with suitable equipment will undertake the study of this region.

The author wishes to acknowledge the assistance of the Hackett Research Studentship granted by the University of Western Australia. His thanks are due to Dr. W. S. Adams, director of the Mount Wilson Observatory, for the use of the Snow telescope, to Dr. S. B. Nicholson, for assistance with the instrumental equipment, and to Mr. H. D. Babcock and Dr. Charlotte E. Moore for extending to him the use of their spectroscopic material not previously published.

CARNEGIE INSTITUTION OF WASHINGTON
MOUNT WILSON OBSERVATORY,
COMMONWEALTH SOLAR OBSERVATORY
CANBERRA
October 1937

THE THEORY OF CYCLICAL TRANSITIONS

L. G. HENYEY

ABSTRACT

The general theory of cyclical transitions in the absence of collisions is discussed, first for a finite number of discrete states. It is found that the rigorous treatment of the radiation field can be carried conveniently to a fairly advanced state, short of the complete solution of the problem. It is found that there exist a number of first integrals of the differential equations, some of which are generalizations of the constancy of the net flux and of the linear dependence of the radiation pressure on the optical depth in the simple scattering problem. The remaining integrals are simple relationships among the optical depths in the various frequencies.

The second part of the discussion is devoted to a study of the properties of the radiation field when the exciting radiation is highly diluted. The approximation appropriate to a high dilution is introduced, and it is found that the problem can be completely solved to within the Milne-Eddington approximation to the directional dependence of the specific intensity. The boundary conditions for a planetary nebula are introduced, and the values of the emergent fluxes are obtained. Physically the approximation for a high dilution is equivalent to neglecting the transitions corresponding to stimulated emissions and those corresponding to absorption when the lower state is not the ground state. However, these facts do not constitute the basis for the approximation; it is introduced from more fundamental considerations.

The last part of the theoretical discussion pertains to the generalization of the theory to an infinite number of discrete states together with a continuum. This formal extension follows in a natural way and depends on no new physical concepts.

Finally there is a section devoted to some computations on the four-state problem for a planetary nebula. One interesting result is the weakness of the (1, 3) radiation (Ly β for hydrogen) when the fourth state is identified with the continuum.

INTRODUCTION

The main features of the problem of the excitation of emission nebulae have been ascertained through the efforts of various investigators. Zanstra's ideas have been widely accepted and are generally regarded as the foundations upon which theoretical investigations must rest. The analytical application of his ideas to a study of the radiative equilibrium of a planetary nebula was first made by Ambarzumian,[1] who considered what can properly be called the three-state problem. The problem was later considered by Chandrasekhar,[2] who traced the conversion of the incident ultraviolet radiation into radiation in Lyman α through the nebular layers.

The problem of the Balmer decrement has been studied theoretically by Cillié[3] and others. The result of these studies has been

[1] *M.N.*, **93**, 50, 1931. Also *Pulk. Obs. Bull.*, No. 13.

[2] *Zs. f. Ap.*, **9**, 266, 1935.

[3] *M.N.*, **96**, 771, 1936.

rather disappointing, in that the agreement with observations was found to be rather poor. It had been found that the lower members of the Balmer series are relatively much more intense than can be expected on the basis of the electron-capture mechanism. An attempt by Berman to remove the discrepancy by correcting for interstellar reddening has shown that the larger part of the differences between observational results and theoretical predictions can be removed but that there still remains some discrepancy.

It is the purpose of the present investigation to provide a more rigorous and systematic treatment of the problem of the radiative equilibrium involving cyclical transitions than has yet been attempted. The discussion has been limited to a nebula in static equilibrium. Although Zanstra[4] has shown that such an object cannot remain in a static state for any length of time, it is nevertheless desirable to obtain as complete a picture as is possible regarding the state of affairs in such a nebula before introducing refinements. This treatment provides the basis for future extensions and gives the correct method of procedure in formulating the problem. It shows, for instance, that the complete treatment of the continuum, or the equilibrium of the electrons, provides no difficulties which differ from what one meets in the treatment of the discrete states.

The investigation is roughly divided into two main sections. In the first section we will study the general relationships concerning the condition of radiative equilibrium and the derivation of several integrals describing the field of radiation. In the second section we will make use of the high dilution of nebular radiations to solve formally the complete representation of the radiation field. It will be convenient at certain stages to regard the continuum as a discrete state, but eventually we will consider the correct method of handling this part of the problem.

This investigation originated from a suggestion made to me by Dr. Chandrasekhar regarding the desirability of a complete and rigorous treatment of the three-state problem in the absence of collision effects. In working on this suggestion, I found that all the explicit relationships which I could derive could be generalized to any number of states, showing that a start can already be made on the

[4] *Ibid.*, **97**, 37, 1936.

more general n-state problem; and, although the work has passed beyond the original suggestion, I am still greatly indebted to Dr. Chandrasekhar for it.

THE EQUATION OF TRANSFER

Let A_{ji}, B_{ji}, and B_{ij} be the Einstein probability co-efficients of spontaneous emission, stimulated emission, and absorption, respectively, defined with respect to the intensity of the radiation. If n_j is the number of atoms in the state (j) per unit volume, the number of downward transitions from state (i) to state (i) is

$$n_j(A_{ji} + \frac{1}{4\pi} B_{ji}\int I_\nu \, d\omega) \tag{1}$$

per unit time and unit volume. The number of upward transitions, under similar circumstances, is

$$\frac{1}{4\pi} n_i B_{ij}\int I_\nu \, d\omega \, . \tag{2}$$

We suppose that the emission and absorption take place within a frequency interval $\Delta\nu_{ij}$, and we consider the average emission and absorption coefficients. The average atomic emission coefficient is

$$\frac{h\nu}{4\pi\Delta\nu_{ij}} A_{ji} \, , \tag{3}$$

the average atomic stimulated emission coefficient is

$$\frac{h\nu}{4\pi\Delta\nu_{ij}} B_{ji} \, , \tag{4}$$

and, finally, the average atomic absorption coefficient is

$$\frac{h\nu}{4\pi\Delta\nu_{ij}} B_{ij} \, . \tag{5}$$

Hence, the equation of transfer becomes

$$\frac{dI_\nu}{ds} = \frac{h\nu}{4\pi\Delta\nu_{ij}} (n_j A_{ji} + n_j B_{ji} I_\nu - n_i B_{ij} I_\nu) \, . \tag{6}$$

We can now make use of the familiar relationships between the various Einstein coefficients, namely,

$$\frac{B_{ij}}{A_{ji}} = \frac{c^2}{2h\nu^3}\frac{g_j}{g_i}, \tag{7}$$

$$\frac{B_{ji}}{A_{ji}} = \frac{c^2}{2h\nu^3}. \tag{8}$$

The quantities g_i are the statistical weights. Eliminating the B's from (6), we find that

$$\frac{dI_\nu}{ds} = g_j A_{ji}\frac{h\nu}{4\pi\Delta\nu_{ij}}\left(\frac{n_j}{g_j} + \left\{\frac{n_j}{g_j} - \frac{n_i}{g_i}\right\}\frac{c^2}{2h\nu^3}I_\nu\right).$$

In the discussion which follows, it is more convenient to describe the radiation field in terms of the flow of photons rather than in terms of the energy flux. Furthermore, we shall use the total intensity over the entire line rather than the intensity per unit frequency interval. We therefore introduce the symbol $\mathcal{J}_{ij}$ defined by the equation

$$\mathcal{J}_{ij} = I_\nu\frac{\Delta\nu_{ij}}{h\nu}, \tag{9}$$

where the subscripts refer to the lower and upper states, respectively. As will become apparent, the ratios n_j/g_j play a more fundamental role than the n's themselves. We denote this ratio by N_j, and we will refer to it as the number of atoms in state (j) per unit volume per unit weight. Finally, we make the abbreviations

$$\frac{1}{4\pi}g_j A_{ji} = \mathcal{B}_{ij}, \tag{10}$$

$$\frac{c^2}{8\pi\nu^2}\frac{g_j A_{ji}}{\Delta\nu_{ij}} = \mu_{ij}. \tag{11}$$

After all these changes the equation of transfer finally becomes

$$\frac{d\mathcal{J}_{ij}}{ds} = \mathcal{B}_{ij}N_j + (N_j - N_i)\mu_{ij}\mathcal{J}_{ij} \tag{12}$$

for transitions between discrete states.

In the case of the bound-free or free-free transitions it is possible to write the equations of transfer in an analogous form. In order to clarify the analysis, we now disregard the continuum and assume temporarily that an atom has only discrete states, and for further simplicity a finite number—say r. Later we shall see that the generalization of the theory offers no difficulties; and, when we do consider these refinements, we shall see that the results follow directly.

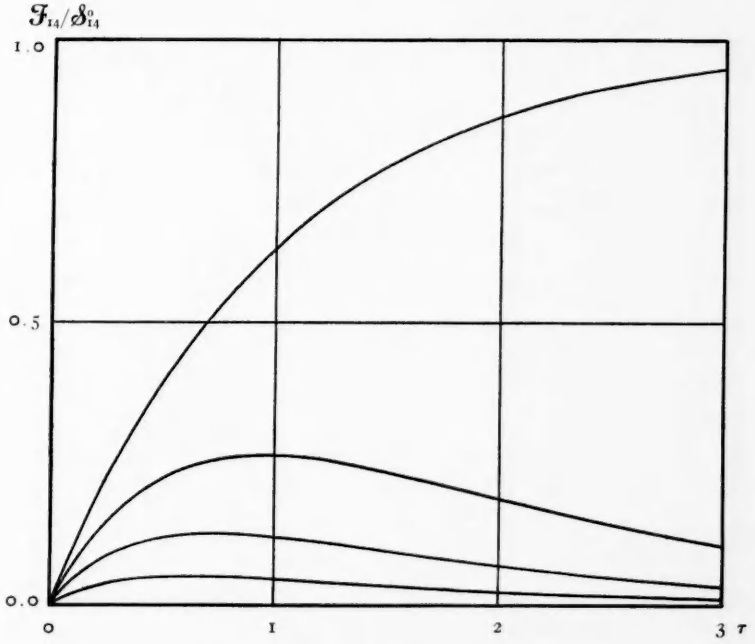

FIG. 1.—From top to bottom the curves correspond to $p_{41} = 1, \frac{3}{4}, \frac{1}{2}, \frac{1}{4}$. These curves also represent $(1 - p_{41})/(p_{43})\mathcal{J}_{34}$, $(1 - p_{41})/(p_{42})\mathcal{J}_{24}$, and $(1 - p_{41})/(p_{43})\mathcal{J}_{23}$.

THE CONDITION OF RADIATIVE EQUILIBRIUM

In order that we may solve (12), it is necessary that we evaluate the N's. Now, the population of the various atomic states is determined in a steady state by the condition of radiative equilibrium. In the case when the gas is mechanically in static equilibrium, this condition is simply the mathematical expression of the fact that at any point the number of transitions into a state during an interval of time is equal to the number of transitions out of this state in the

same interval of time, all transitions taking place spontaneously or under the influence of radiation. If we write

$$\mathcal{J}_{ij} = \int \mathcal{I}_{ij} \frac{d\omega}{4\pi}, \tag{13}$$

where the integration is performed over all directions, we have for the condition of radiative equilibrium

$$\sum_{j=1}^{i-1} N_j \mu_{ji} \mathcal{J}_{ji} + \sum_{j=i+1}^{r} N_i (\mathcal{B}_{ij} + \mu_{ij} \mathcal{J}_{ij}) = \sum_{j=1}^{i-1} N_i (\mathcal{B}_{ji} + \mu_{ji} \mathcal{J}_{ji}) + \sum_{i=i+1}^{r} N_i \mu_{ij} \mathcal{J}_{ij}.$$

Rearranging the terms, we have

$$\left.\begin{aligned} \sum_{j=1}^{i-1} (N_i \mathcal{B}_{ji} + \{N_i - N_j\} \mu_{ji} \mathcal{J}_{ji}) \\ - \sum_{j=i+1}^{r} (N_i \mathcal{B}_{ij} + \{N_j - N_i\} \mu_{ij} \mathcal{J}_{ij}) = 0. \end{aligned}\right\} \tag{14}$$

The equations in (14) are not all linearly independent, for, if we sum over all possible values of (i), we get identically zero. The equations serve in principle to calculate the ratios of the N's in terms of the intensities in the radiation field. Obviously, an explicit solution of (14) will be exceedingly complicated. However, various general integrals of the differential equations of the radiation field can be obtained without solving the equations of radiative equilibrium.

The operator d/ds, occurring in the equation of transfer, can be expanded into the well-known form

$$l \frac{\partial}{\partial x} + m \frac{\partial}{\partial y} + n \frac{\partial}{\partial z},$$

where (l, m, n) are the direction cosines of the ray. The vectorial net photon flux $\pi \mathcal{F}_{ij}$ has components given by

$$\mathcal{F}_{x,\,ij} = \int \mathcal{I}_{ij} l \frac{d\omega}{\pi}, \qquad \mathcal{F}_{y,\,ij} = \int \mathcal{I}_{ij}\, m \frac{d\omega}{\pi}, \qquad \mathcal{F}_{z,\,ij} = \int \mathcal{I}_{ij} n \frac{d\omega}{\pi}. \tag{15}$$

An integration over all solid angles of both sides of (12) leads to the result

$$\left.\begin{aligned} \tfrac{1}{4}\operatorname{div}\mathfrak{F}_{ij} = \frac{1}{4}\left(\frac{\partial \mathfrak{F}_{x,\,ij}}{\partial x} + \frac{\partial \mathfrak{F}_{y,\,ij}}{\partial y} + \frac{\partial \mathfrak{F}_{z,\,ij}}{\partial z}\right) \\ = \mathfrak{B}_{ij}N_j + (N_j - N_i)\mu_{ij}\mathfrak{J}_{ij}\,. \end{aligned}\right\} \tag{16}$$

Consequently, by (14),

$$\operatorname{div}\left(\sum_{j=1}^{i-1}\mathfrak{F}_{ji} - \sum_{j=i+1}^{r}\mathfrak{F}_{ij}\right) = 0\,. \tag{17}$$

If the material is stratified in parallel planes, (17) becomes, for the fluxes normal to the plane of stratification,

$$\frac{d}{dz}\left(\sum_{j=1}^{i-1}\mathfrak{F}_{ji} - \sum_{j=i+1}^{r}\mathfrak{F}_{ij}\right) = 0\,,$$

where z is the co-ordinate whose variation is normal to the planes of stratification. Hence,

$$\sum_{j=1}^{i-1}\mathfrak{F}_{ji} - \sum_{j=i+1}^{r}\mathfrak{F}_{ij} = a_i\,. \tag{18}$$

If the system has spherical symmetry, we can deduce from (17) that for the radial fluxes,

$$\sum_{j=1}^{i-1}\mathfrak{F}_{ji} - \sum_{j=i+1}^{r}\mathfrak{F}_{ij} = \frac{a_i}{r^2}\,, \tag{19}$$

where r is the distance from the center of symmetry. In general,

$$\sum_{j=1}^{i-1}\mathfrak{F}_{ji} - \sum_{j=i+1}^{r}\mathfrak{F}_{ij} = \operatorname{curl}\mathbf{A}_i\,, \tag{20}$$

where $\mathbf{A}_i$ is an arbitrary vector field. These relationships, which we will call the *flux integrals*, constitute the generalization of the familiar constancy of the net flux in the pure scattering problem. Not all of these integrals are independent, for, if we sum them over

all the states, we have identically zero. Hence, there are $r - 1$ independent relationships.

While the equations (18), (19), and (20) are concerned with the photon flow, they guarantee the conservation of energy in the radia-

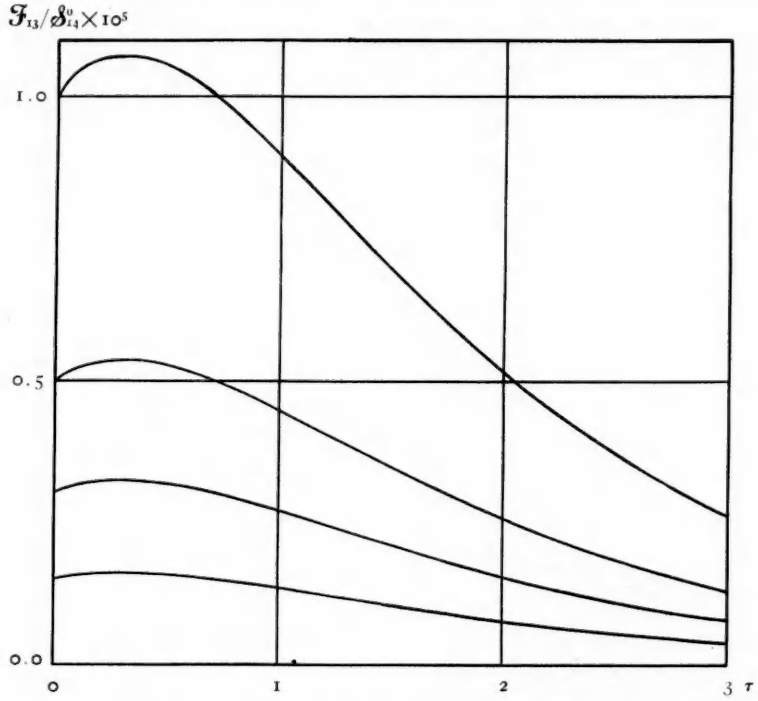

FIG. 2.—$p_{41} = \frac{3}{4}$. From top to bottom we have p_{42} and p_{31} equal to $(0, \frac{2}{3})$, $(\frac{1}{8}, \frac{2}{3})$, $(0, \frac{1}{3})$, $(\frac{1}{8}, \frac{1}{3})$.

tion field as in the simple scattering problem. The total energy flux is proportional to

$$\sum_{i=1}^{r-1} \sum_{j=i+1}^{r} \nu_{ij} \mathcal{F}_{ij} .$$

From the Bohr frequency relation this equals

$$\sum_{i=1}^{r-2} \sum_{j=i+1}^{r-1} (\nu_{ir} - \nu_{jr}) \mathcal{F}_{ij} + \sum_{i=1}^{r-1} \nu_{ir} \mathcal{F}_{ir} .$$

Rearranging the terms in the double summation, this reduces to

$$\sum_{i=1}^{r-1} \nu_{ir} \left(-\sum_{j=1}^{i-1} \mathcal{F}_{ji} + \sum_{j=i+1}^{r} \mathcal{F}_{ij} \right).$$

From (17) it can be seen that the divergence of this expression is zero. This proves the proposition.

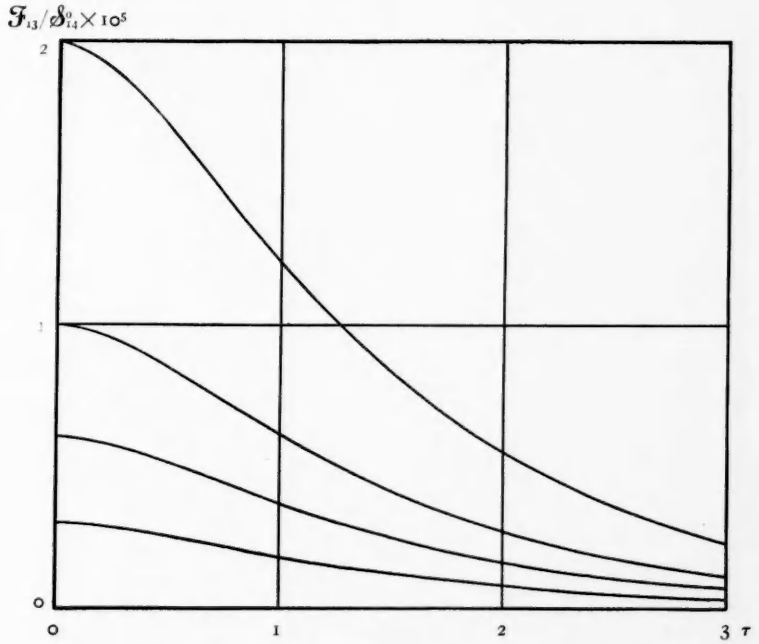

FIG. 3.—$p_{41} = \frac{1}{2}$. From top to bottom we have p_{42} and p_{31} equal to $(0, \frac{2}{3})$, $(\frac{1}{4}, \frac{2}{3})$, $(0, \frac{1}{3})$, $(\frac{1}{4}, \frac{1}{3})$.

The optical depth τ_{ij} along a ray in the (ij) radiation is defined by

$$d\tau_{ij} = (N_j - N_i)\mu_{ij} ds . \qquad (21)$$

For any three states (i, j, and k) such that $i < j < k$, it follows immediately from (21) that

$$d\left(\frac{\tau_{ij}}{\mu_{ij}} + \frac{\tau_{jk}}{\mu_{jk}} - \frac{\tau_{ik}}{\mu_{ik}} \right) = 0$$

along the ray. Or,

$$\frac{\tau_{ij}}{\mu_{ij}} + \frac{\tau_{jk}}{\mu_{jk}} - \frac{\tau_{ik}}{\mu_{ik}} = 0 , \tag{22}$$

provided they are all measured from the same point. We shall refer to these as the *τ-integrals*. Now, if we write (22) for all possible sets of three states, not all the equations will be independent. In fact, there are only $[(r-1)(r-2)]/2$ independent integrals. To see this, let us consider the set of equations

$$\frac{\tau_{1j}}{\mu_{1j}} + \frac{\tau_{jk}}{\mu_{jk}} - \frac{\tau_{1k}}{\mu_{1k}} = 0 . \qquad (1 < j < k \leq r) .$$

This set contains only such equations as are independent, since only one of them has the term τ_{jk}/μ_{jk}, and it contains exactly $[(r-1)(r-2)]/2$ equations. Now, any combination of three states other than those represented in this set leads to an integral which can be derived from those in the set, for

$$\frac{\tau_{ij}}{\mu_{ij}} + \frac{\tau_{jk}}{\mu_{jk}} - \frac{\tau_{ik}}{\mu_{ik}} = \left(\frac{\tau_{1i}}{\mu_{1i}} + \frac{\tau_{ij}}{\mu_{ij}} - \frac{\tau_{1j}}{\mu_{1j}}\right) + \left(\frac{\tau_{1j}}{\mu_{1j}} + \frac{\tau_{jk}}{\mu_{jk}} - \frac{\tau_{1k}}{\mu_{1k}}\right) - \left(\frac{\tau_{1i}}{\mu_{1i}} + \frac{\tau_{ik}}{\mu_{ik}} - \frac{\tau_{1k}}{\mu_{1k}}\right) , \quad (1 < i < j < k \leq r) ,$$

proving the proposition.

Now, suppose that $\bar{\mathcal{J}}_{ij}$ represents the intensity of the incident illumination after passage through a portion of the nebula. Then, along a ray,

$$\frac{d\bar{\mathcal{J}}_{ij}}{ds} = (N_j - N_i)\mu_{ij}\bar{\mathcal{J}}_{ij} . \tag{23}$$

Hence,

$$\bar{\mathcal{J}}_{ij} = \bar{\mathcal{J}}^0_{ij}\, e^{-(\tau^0_{ij} - \tau_{ij})} , \tag{24}$$

where the zero superscripts refer to the surface at which the incident radiation enters the nebula. The τ-integrals can be written in the alternate form:

$$\frac{1}{\mu_{ij}} \log \frac{\bar{\mathcal{J}}_{ij}}{\bar{\mathcal{J}}^0_{ij}} + \frac{1}{\mu_{jk}} \log \frac{\bar{\mathcal{J}}_{jk}}{\bar{\mathcal{J}}^0_{jk}} - \frac{1}{\mu_{ik}} \log \frac{\bar{\mathcal{J}}_{ik}}{\bar{\mathcal{J}}^0_{ik}} = 0 . \tag{25}$$

In a preceding paragraph we considered the generalization of the flux integral in the simple scattering problem. By virtue of these relationships we are able to derive one other integral which is a gener-

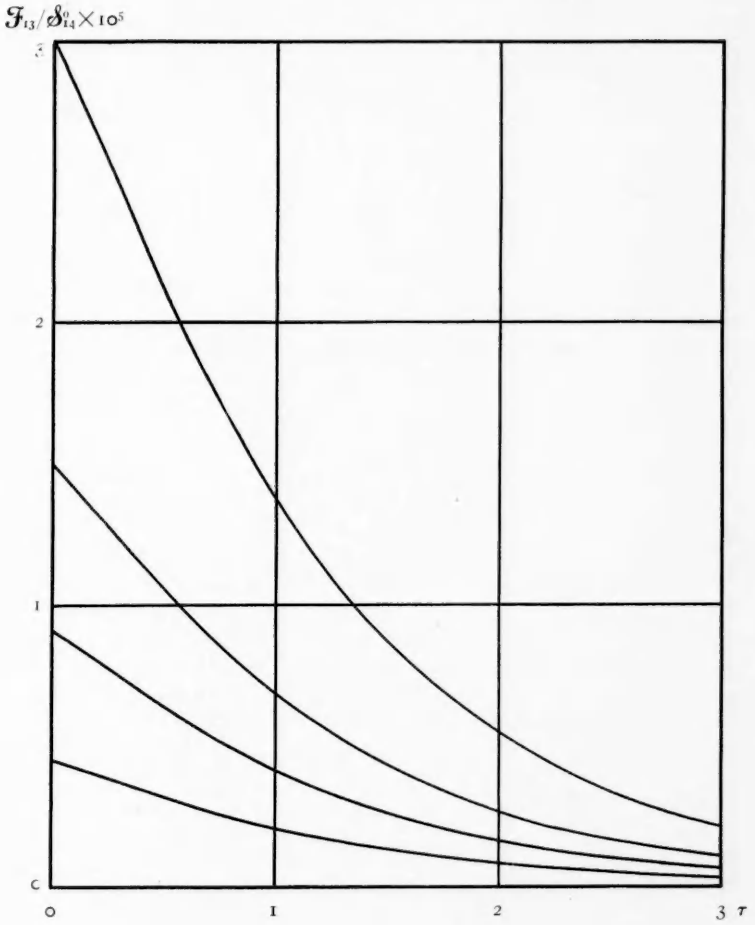

FIG. 4.—$p_{41} = \frac{1}{4}$. From top to bottom we have p_{42} and p_{31} equal to $(0, \frac{2}{3})$, $(\frac{3}{8}, \frac{2}{3})$, $(0, \frac{1}{3})$, $(\frac{3}{8}, \frac{1}{3})$.

alization of another relationship in the theory of simple scattering—the well-known[5] linear dependence of the pressure on the optical depth. The possibility of generalizing this integral was suggested to

[5] Cf. Milne, *Handbuch d. Ap.*, **3**, Eq. 125.

the author by Dr. Chandrasekhar, who found a special form of the generalization in his study of the three-state problem. In deriving the integral we limit ourselves to the case of plane-parallel stratification. Then we have

$$\cos\theta \frac{d\mathcal{I}_{ij}}{dz} = \mathcal{B}_{ij}N_j + (N_j - N_i)\mu_{ij}\mathcal{I}_{ij} . \tag{26}$$

Since

$$\left.\begin{aligned} \mathcal{J}_{ij} &= \frac{1}{2}\int_0^\pi \mathcal{I}_{ij} \sin\theta d\theta , \\ \mathcal{F}_{ij} &= 2\int_0^\pi \mathcal{I}_{ij} \sin\theta\cos\theta d\theta , \\ \mathcal{K}_{ij} &= \frac{1}{2}\int_0^\pi \mathcal{I}_{ij} \sin\theta\cos^2\theta d\theta , \end{aligned}\right\} \tag{27}$$

we have

$$\left.\begin{aligned} \frac{1}{4}\frac{d\mathcal{F}_{ij}}{dz} &= \mathcal{B}_{ij}N_j + (N_j - N_i)\mu_{ij}\mathcal{J}_{ij} , \\ \frac{d\mathcal{K}_{ij}}{dz} &= \tfrac{1}{4}(N_j - N_i)\mu_{ij}\mathcal{F}_{ij} . \end{aligned}\right\} \tag{28}$$

From the second of these,

$$\frac{d}{dz}\sum_{i=1}^{r}\sum_{j=i+1}^{r}\frac{1}{\mu_{ij}}\mathcal{K}_{ij} = \frac{1}{4}\sum_{i=1}^{r}\sum_{j=i+1}^{r}(N_j - N_i)\mathcal{F}_{ij} .$$

After some reduction the right-hand side becomes

$$\frac{1}{4}\sum_{i=1}^{r}N_i\left\{\sum_{j=1}^{i-1}\mathcal{F}_{ji} - \sum_{j=i+1}^{r}\mathcal{F}_{ij}\right\} .$$

From the flux integrals this equals

$$\frac{1}{4}\sum_{i=1}^{r} N_i \left\{ \sum_{j=1}^{i-1} \mathcal{F}_{ji}^{o} - \sum_{j=i+1}^{r} \mathcal{F}_{ij}^{o} \right\} ,$$

where the superscripts refer to the values of the quantities at some arbitrary but fixed value of z. If we reverse the reduction, this becomes

$$\frac{1}{4}\sum_{i=1}^{r}\sum_{j=i+1}^{r} (N_j - N_i)\mathcal{F}_{ij}^{o} .$$

From the definition of the optical depth the equation becomes

$$\frac{d}{dz}\sum_{i=1}^{r}\sum_{j=i+1}^{r}\frac{1}{\mu_{ij}}\mathcal{K}_{ij} = \frac{1}{4}\frac{d}{dz}\sum_{i=1}^{r}\sum_{j=i+1}^{r}\frac{\tau_{ij}}{\mu_{ij}}\mathcal{F}_{ij}^{o} .$$

Integrating, we finally have the K-*integral*,

$$\sum_{i,j}\frac{1}{\mu_{ij}}(\mathcal{K}_{ij} - \tfrac{1}{4}\mathcal{F}_{ij}^{o}\tau_{ij}) = \text{constant} . \qquad (29)$$

In concluding this section, we remark that we have found $r - 1$ independent flux integrals, $[(r-1)(r-2)]/2$ independent τ-integrals, and one K-integral, giving a total of $(r^2 - 3r + 4)/2$ independent integrals.

THE THREE-STATE PROBLEM

As an example of the preceding analysis and for use in later sections of this paper, in this section we formulate the three-state problem for a plane-parallel model with perpendicularly incident radiation.

The condition of radiative equilibrium gives rise to the two equations:

$$(\mu_{12}\mathcal{J}_{12} + \mu_{13}\mathcal{J}_{13})N_1 - (\mathcal{B}_{12} + \mu_{12}\mathcal{J}_{12})N_2 - (\mathcal{B}_{13} + \mu_{13}\mathcal{J}_{13})N_3 = 0 ,$$
$$-\mu_{12}\mathcal{J}_{12}N_1 + (\mathcal{B}_{12} + \mu_{12}\mathcal{J}_{12} + \mu_{23}\mathcal{J}_{23})N_2 - (\mathcal{B}_{23} + \mu_{23}\mathcal{J}_{23})N_3 = 0 .$$

Solving for the ratios of the N's, we have

$$\left.\begin{aligned} N_1 \propto\ & \mathcal{B}_{12}(\mathcal{B}_{13}+\mathcal{B}_{23}) + (\mathcal{B}_{13}+\mathcal{B}_{23})\mu_{12}\mathcal{J}_{12} \\ & + \mathcal{B}_{12}\mu_{13}\mathcal{J}_{13} + (\mathcal{B}_{12}+\mathcal{B}_{13})\mu_{23}\mathcal{J}_{23} + \mu_{12}\mu_{13}\mathcal{J}_{12}\mathcal{J}_{13} \\ & + \mu_{12}\mu_{23}\mathcal{J}_{12}\mathcal{J}_{23} + \mu_{13}\mu_{23}\mathcal{J}_{13}\mathcal{J}_{23}\,, \\ N_2 \propto\ & (\mathcal{B}_{13}+\mathcal{B}_{23})\mu_{12}\mathcal{J}_{12} + \mathcal{B}_{23}\mu_{13}\mathcal{J}_{13} + \mu_{12}\mu_{13}\mathcal{J}_{12}\mathcal{J}_{13} \\ & + \mu_{12}\mu_{23}\mathcal{J}_{12}\mathcal{J}_{23} + \mu_{13}\mu_{23}\mathcal{J}_{13}\mathcal{J}_{23}\,, \\ N_3 \propto\ & \mathcal{B}_{12}\mu_{13}\mathcal{J}_{13} + \mu_{12}\mu_{13}\mathcal{J}_{12}\mathcal{J}_{13} + \mu_{12}\mu_{23}\mathcal{J}_{12}\mathcal{J}_{23} + \mu_{13}\mu_{23}\mathcal{J}_{13}\mathcal{J}_{23}\,. \end{aligned}\right\} \tag{30}$$

Next, we need the quantities

$$\left.\begin{aligned} N_1 - N_2 \propto\ & \mathcal{B}_{12}(\mathcal{B}_{13}+\mathcal{B}_{23}) + (\mathcal{B}_{12}-\mathcal{B}_{23})\mu_{13}\mathcal{J}_{13} \\ & + (\mathcal{B}_{12}+\mathcal{B}_{13})\mu_{23}\mathcal{J}_{23}\,, \\ N_1 - N_3 \propto\ & \mathcal{B}_{12}(\mathcal{B}_{13}+\mathcal{B}_{23}) + (\mathcal{B}_{13}+\mathcal{B}_{23})\mu_{12}\mathcal{J}_{12} \\ & + (\mathcal{B}_{12}+\mathcal{B}_{13})\mu_{23}\mathcal{J}_{23}\,, \\ N_2 - N_3 \propto\ & (\mathcal{B}_{13}+\mathcal{B}_{23})\mu_{12}\mathcal{J}_{12} - (\mathcal{B}_{12}-\mathcal{B}_{23})\mu_{13}\mathcal{J}_{13}\,. \end{aligned}\right\} \tag{31}$$

From these equations and (28)

$$\left.\begin{aligned} \frac{1}{4}\frac{d\mathcal{F}_{12}}{dz} = -\frac{1}{4}\frac{d\mathcal{F}_{13}}{dz} = \frac{1}{4}\frac{d\mathcal{F}_{23}}{dz} \propto\ & \mathcal{B}_{12}\mathcal{B}_{23}\mu_{13}\mathcal{J}_{13} + \mathcal{B}_{23}\mu_{12}\mu_{13}\mathcal{J}_{12}\mathcal{J}_{13} \\ & - \mathcal{B}_{13}\mu_{12}\mu_{23}\mathcal{J}_{12}\mathcal{J}_{23} + \mathcal{B}_{12}\mu_{13}\mu_{23}\mathcal{J}_{13}\mathcal{J}_{23} \end{aligned}\right\} \tag{32}$$

and

$$\left.\begin{aligned} \frac{d\mathcal{K}_{12}}{dz} \propto\ & -\tfrac{1}{4}\{\mathcal{B}_{12}(\mathcal{B}_{13}+\mathcal{B}_{23}) + (\mathcal{B}_{12}-\mathcal{B}_{23})\mu_{13}\mathcal{J}_{13} \\ & + (\mathcal{B}_{12}+\mathcal{B}_{13})\mu_{23}\mathcal{J}_{23}\}\mu_{12}\mathcal{F}_{12}\,, \\ \frac{d\mathcal{K}_{13}}{dz} \propto\ & -\tfrac{1}{4}\{\mathcal{B}_{12}(\mathcal{B}_{13}+\mathcal{B}_{23}) + (\mathcal{B}_{13}+\mathcal{B}_{23})\mu_{12}\mathcal{J}_{12} \\ & + (\mathcal{B}_{12}+\mathcal{B}_{13})\mu_{23}\mathcal{J}_{23}\}\mu_{13}\mathcal{F}_{13}\,, \\ \frac{d\mathcal{K}_{23}}{dz} \propto\ & -\tfrac{1}{4}\{(\mathcal{B}_{13}+\mathcal{B}_{23})\mu_{12}\mathcal{J}_{12} - (\mathcal{B}_{12}-\mathcal{B}_{23})\mu_{13}\mathcal{J}_{13}\}\mu_{23}\mathcal{F}_{23}\,. \end{aligned}\right\} \tag{33}$$

The normal optical depths are defined by

$$\left.\begin{aligned}
\frac{1}{\mu_{12}}\frac{d\tau_{12}}{dz} &\propto -\mathcal{B}_{12}(\mathcal{B}_{13}+\mathcal{B}_{23}) - (\mathcal{B}_{12}-\mathcal{B}_{23})\mu_{13}\mathcal{J}_{13} \\
&\qquad - (\mathcal{B}_{12}+\mathcal{B}_{13})\mu_{23}\mathcal{J}_{23}\,, \\
\frac{1}{\mu_{13}}\frac{d\tau_{13}}{dz} &\propto -\mathcal{B}_{12}(\mathcal{B}_{13}+\mathcal{B}_{23}) - (\mathcal{B}_{13}+\mathcal{B}_{23})\mu_{12}\mathcal{J}_{12} \\
&\qquad - (\mathcal{B}_{12}+\mathcal{B}_{13})\mu_{23}\mathcal{J}_{23}\,, \\
\frac{1}{\mu_{23}}\frac{d\tau_{23}}{dz} &\propto -(\mathcal{B}_{13}+\mathcal{B}_{23})\mu_{12}\mathcal{J}_{12} + (\mathcal{B}_{12}-\mathcal{B}_{23})\mu_{13}\mathcal{J}_{13}\,.
\end{aligned}\right\} \tag{34}$$

The factor of proportionality is the same in all of the preceding equations. Equations (30) show that this factor is always positive and different from zero, so that, if we denote it by Δ,

$$\frac{du}{dz} = \Delta$$

determines a function $u(z)$ which is monotone increasing. Hence, we can use it as the independent variable; and by substituting it for z, we can replace all of the proportionality signs in equations (32) to (34) by equality signs.

In order to complete the formulation of the problem we must introduce the Milne-Eddington approximation. If there is incident radiation which is concentrated in a small solid angle, we must separate it from the diffuse radiation before we apply the approximation. If we denote the incident photon flux by $\pi\mathcal{S}_{ij}$, and if the rays are along the positive z direction, we have that the $\mathcal{J}_{ij}$ and the $\mathcal{K}_{ij}$ for the incident light is equal to $\mathcal{S}_{ij}$. Therefore, the correct approximation is

$$3(\mathcal{K}_{ij} - \tfrac{1}{4}\mathcal{S}_{ij}) = \mathcal{J}_{ij} - \tfrac{1}{4}\mathcal{S}_{ij}\,,$$

or

$$\mathcal{K}_{ij} = \tfrac{1}{3}\mathcal{J}_{ij} + \tfrac{1}{6}\mathcal{S}_{ij}\,. \tag{35}$$

In general, when the third state is identified with the continuum, the diffuse radiation will be determined largely by $\mathcal{S}_{13}$. It is of inter-

est to consider the case of both $\mathcal{S}_{12}$ and $\mathcal{S}_{23}$ equal to zero in the planetary problem, since we can establish another integral under these circumstances. From the flux integrals or from (42) we see that $\mathcal{F}_{12}$ and $\mathcal{F}_{13}$ differ only by a constant. Since the diffuse fluxes must be zero on the inner boundary of a planetary nebula, it follows that this constant difference must be zero. Therefore, by straightforward substitution we have from (32) and (33)

$$\tfrac{1}{16}(\mathcal{B}_{12} - \mathcal{B}_{23})\mathcal{F}_{12}\frac{d\mathcal{F}_{12}}{du} + \mathcal{B}_{23}\mathcal{J}_{12}\frac{d\mathcal{K}_{12}}{du} - \mathcal{B}_{12}\left(\mathcal{J}_{23} + \frac{\mathcal{B}_{23}}{\mu_{23}}\right)\frac{d\mathcal{K}_{23}}{du} = 0 .$$

Using the approximation (35), when $\mathcal{S}_{12} = \mathcal{S}_{23} = 0$, we have

$$\frac{1}{16}\left(\frac{1}{\mathcal{B}_{23}} - \frac{1}{\mathcal{B}_{12}}\right)\mathcal{F}_{12}^2 + \frac{1}{3\mathcal{B}_{12}}\mathcal{J}_{12}^2 - \frac{1}{3\mathcal{B}_{23}}\left(\mathcal{J}_{23} + \frac{\mathcal{B}_{23}}{\mu_{23}}\right)^2 = \text{constant} . \qquad (36)$$

A special form of this integral has been derived by Chandrasekhar.

THE NEBULAR PROBLEM

In the preceding discussion we have not concerned ourselves with the essential property of nebular radiation, namely, its high dilution. If the incident light is roughly distributed according to dilute blackbody radiation, this high dilution implies that

$$\frac{c^2}{2h\nu^3} I_\nu \ll 1 ,$$

except in the extremely long wave-length region of the spectrum. In our notation this inequality becomes

$$\frac{\mu_{ij}}{\mathcal{B}_{ij}}\mathcal{J}_{ij} \ll 1 . \qquad (37)$$

Now, in the nebula the incident radiation is redistributed over different parts of the spectrum, the most striking being the enormous gain of Ly α in the diffuse radiation over the direct. This gain probably

does not exceed 10^4 or, if the Doppler broadening of the lines is lower than is usually accepted, 10^5. However, this gain is hardly sufficient in the great majority of planetary or diffuse galactic nebulae to neutralize the smallness of the dilution factor, which lies in the range $<10^{-9}$.[6] Even in Be or Wolf-Rayet stars, where the dilution factor is not as extreme as in nebulae, an important first approximation to the actual situation can be worked out on the basis of (37). The importance of the inequality lies in the fact that it enables us to solve the conditions of radiative equilibrium explicitly in a very satisfactory form.

An examination of the complete solution (30) for the three-state problem gives the clue to the form of the general solution. Applying (37) and remembering that $\mathcal{B}_{23} \sim \mathcal{B}_{12}$, as far as order of magnitude is concerned, we have

$$\frac{N_2}{N_1} = \frac{\mu_{12}}{\mathcal{B}_{12}} \mathcal{J}_{12} + \frac{\mathcal{B}_{23}\mu_{13}}{\mathcal{B}_{12}(\mathcal{B}_{13} + \mathcal{B}_{23})} \mathcal{J}_{13} ,$$

$$\frac{N_3}{N_1} = \frac{\mu_{13}}{\mathcal{B}_{13} + \mathcal{B}_{23}} \mathcal{J}_{13} .$$

These values suggest the following generalization ($j > 1$) for r states:

$$\frac{N_j}{N_1} = \gamma_j \frac{\mu_{1j}}{\mathcal{B}_{1j}} \mathcal{J}_{1j} + \sum_{l=j+1}^{r} \gamma_{jl} \frac{\mu_{1l}}{\mathcal{B}_{1l}} \mathcal{J}_{1l} . \tag{38}$$

To determine the coefficients in (38) we substitute these equations into (14). Retaining only first-order terms, (14) (for $i > 1$) becomes, after some rearranging,

$$\left\{ \frac{\gamma_i}{\mathcal{B}_{1i}} \sum_{j=1}^{i-1} \mathcal{B}_{ji} - 1 \right\} \mu_{1i}\mathcal{J}_{1i} + \sum_{l=i+1}^{r} \mu_{1l}\mathcal{J}_{1l} \left\{ \frac{\gamma_{il}}{\mathcal{B}_{1l}} \sum_{j=1}^{i-1} \mathcal{B}_{ji} - \frac{\mathcal{B}_{il}\gamma_l}{\mathcal{B}_{1l}} - \sum_{j=i+1}^{l-1} \frac{\mathcal{B}_{ij}\gamma_{jl}}{\mathcal{B}_{1l}} \right\} = 0 .$$

[6] This argument is essentially due to Ambarzumian, *M.N.*, **95**, 469, 1935.

Each of these equations is satisfied by equating the coefficients of each of the $\mathcal{J}$'s to zero. Doing this, we obtain the following recurrence formulae for the coefficients in (38):

$$\gamma_i = \frac{\mathcal{B}_{1i}}{\sum_{j=1}^{i-1} \mathcal{B}_{ji}}, \tag{39}$$

$$\gamma_{il} = \frac{1}{\sum_{j=1}^{i-1} \mathcal{B}_{ji}} \left\{ \mathcal{B}_{il}\gamma_l + \sum_{j=i+1}^{l-1} \mathcal{B}_{ij}\gamma_{jl} \right\}. \tag{40}$$

Now let

$$p_{ji} = \frac{\mathcal{B}_{ij}}{\sum_{k=1}^{j-1} \mathcal{B}_{kj}}, \qquad p_{j1} = \frac{\mathcal{B}_{1j}}{\sum_{k=1}^{j-1} \mathcal{B}_{kj}} = \gamma_j, \tag{41}$$

and let

$$\gamma_{il} = \frac{\mathcal{B}_{1l}}{\sum_{k=1}^{i-1} \mathcal{B}_{ki}} q_{li}. \tag{42}$$

From (41),

$$\sum_{i=1}^{j-1} p_{ji} = 1.$$

We can readily see that p_{ji} is the probability that an atom, undergoing a spontaneous transition from a state (j), will pass directly into the state (i). From (40), (41), and (42)

$$q_{li} = p_{li} + \sum_{j=i+1}^{j-1} q_{lj} p_{ji}. \tag{43}$$

Now consider the probability, analogous to p_{ji}, that the atom, after leaving (j), will arrive eventually in (i) after an arbitrary number of

downward transitions. But these probabilities must satisfy recurrence formulae identical with (43) if we identify them with the q's. Therefore, q_{ji} is, in fact, this quantity.

Equation (38) can be written in the form

$$\frac{N_j}{N_1}\sum_{k=1}^{j-1}\mathcal{B}_{kj} = \mu_{1j}\mathcal{J}_{1j} + \sum_{l=j+1}^{r} q_{lj}\mu_{1l}\mathcal{J}_{1l}\,. \tag{44}$$

Equation (44) is precisely what we should expect if the effect of transitions, corresponding to absorption and stimulated emissions and not involving the ground state, is negligible. For the terms on the right-hand side give the frequency with which atoms arrive into state (j), owing to absorptions in the principal series, whereas the term on the left represents the frequency of departure. This explanation of (44) is the underlying principle in recent calculations of the theoretical Balmer decrement.

Having determined the population of each state, we can now calculate the intensities in the radiation field. The first step is the investigation of the transitions involving the ground state. The emission coefficient for the case of a discrete upper state is

$$\mathcal{B}_{1j}N_j = N_1 p_{j1}\left\{\mu_{1j}\mathcal{J}_{1j} + \sum_{l=j+1}^{r} q_{lj}\mu_{1l}\mathcal{J}_{1l}\right\}. \tag{45}$$

The absorption coefficients are

$$(N_1 - N_j)\mu_{1j} \sim N_1\mu_{1j}\,,$$

by virtue of the fact that N_j/N_1 is small. Hence, for a medium stratified in parallel planes,

$$\frac{1}{4}\frac{d\mathcal{F}_{1j}}{dt} = \sum_{k=j}^{r}\beta_{kj}\mu_{1k}\mathcal{J}_{1k} - \mu_j\mathcal{J}_{1j}\,,$$

where

$$t = \int N_1 dz$$

and

$$\beta_{kj} = q_{kj}p_{j1}, \qquad \beta_{jj} = p_{j1}. \tag{46}$$

It is convenient to separate the incident and the diffuse intensities. Let us denote the quantities that refer to the total intensity by means of an asterisk. Hence,

$$\left.\begin{aligned} \mathcal{J}^*_{ij} &= \mathcal{J}_{ij} + \tfrac{1}{4}\mathcal{S}_{ij}, \\ \mathcal{F}^*_{ij} &= \mathcal{F}_{ij} + \mathcal{S}_{ij}, \\ \mathcal{K}^*_{ij} &= \mathcal{K}_{ij} + \tfrac{1}{4}\mathcal{S}_{ij}, \end{aligned}\right\} \tag{47}$$

where $\pi\mathcal{S}_{ij}$ is the net flux in the incident radiation. We have for our complete system, using the Milne-Eddington approximation and dropping the subscript 1,

$$\left.\begin{aligned} \tfrac{1}{4}\frac{d\mathcal{F}_j}{dt} &= \sum_{k=j}^{r} \beta_{kj}\mu_k(\mathcal{J}_k + \tfrac{1}{4}\mathcal{S}_k) - \mu_j\mathcal{J}_j, \\ \frac{d\mathcal{J}_j}{dt} &= -\tfrac{3}{4}\mu_j\mathcal{F}_j, \\ \frac{d\mathcal{S}_j}{dt} &= -\mu_j\mathcal{S}_j. \end{aligned}\right\} \tag{48}$$

Since the equations are linear, we can make another simplification. We suppose that all the incident intensities are zero except $\mathcal{S}_r$. The complete solution is simply the sum of all these special solutions with r taking all possible values.

Eliminating $\mathcal{F}_j$ from (48), and writing

$$\lambda_j^2 = 3\mu_j^2(1 - \beta_{jj}),$$

we have

$$\frac{d^2\mathcal{J}_j}{dt^2} - \lambda_j^2\mathcal{J}_j = -3\mu_j \sum_{k=j+1}^{r} \beta_{kj}\mu_k\mathcal{J}_k - \tfrac{3}{4}\beta_{rj}\mu_j\mu_r\mathcal{S}_r. \tag{49}$$

We try a solution of the form

$$\mathcal{J}_j = \frac{3\mu_j}{\lambda_j}\{A_j e^{\lambda j t} + B_j e^{-\lambda j t}\} + \mu_j \sum_{k=j+1}^{r} \frac{a_{jk}}{\mu_k}\mathcal{J}_k + \frac{3\mu_j}{4\mu_r} a_j \mathcal{S}_r . \quad (50)$$

Now

$$\frac{d^2\mathcal{J}_k}{dt^2} - \lambda_j^2 \mathcal{J}_k = (\lambda_k^2 - \lambda_j^2)\mathcal{J}_k - 3\mu_k \sum_{l=k+1}^{r} \beta_{lk}\mu_l \mathcal{J}_l - \tfrac{3}{4}\mu_k^{\mu_r}\beta_{rk}\mathcal{S}_r .$$

Using this equation and introducing (50) into (49), we find that

$$\frac{d^2\mathcal{J}_j}{dt^2} - \lambda_j^2 \mathcal{J}_j = \mu_j \sum_{k=j+1}^{r} \mu_k \mathcal{J}_k \left\{ \frac{a_{jk}}{\mu_k^2}(\lambda_k^2 - \lambda_j^2) - 3\sum_{l=j+1}^{k-1} a_{jl}\beta_{kl} \right\}$$
$$+ \tfrac{3}{4}\mu_j \mu_r \mathcal{S}_r \left\{ \frac{a_j}{\mu_r^2}(\mu_r^2 - \lambda_j^2) - \sum_{k=j+1}^{r} a_{jk}\beta_{rk} \right\} .$$

To satisfy (49) we equate the coefficients of $\mathcal{J}_k$ and $\mathcal{S}_r$ in (49) to those in the preceding equation. From this we derive the recurrence formula

$$a_{jk} = \frac{3\mu_k^2}{\lambda_j^2 - \lambda_k^2}\left\{ \beta_{kj} - \sum_{l=j+1}^{k-1} a_{jl}\beta_{kl} \right\}, \quad (51)$$

and the formula

$$a_j = \frac{\mu_r^2}{\lambda_j^2 - \mu_r^2}\left\{ \beta_{rj} - \sum_{l=j+1}^{r} a_{jl}\beta_{rl} \right\}. \quad (52)$$

It follows that the solution of the differential equations (48) can be expanded into (50) provided that no two of the λ's are equal and provided that no λ is equal to μ_r. When these conditions are not satisfied, it is necessary to introduce polynomial terms in t into the solution. We will not consider these degenerate cases separately, since, as is well known, their solutions can be derived from the non-degenerate solution after the boundary conditions have been assigned.

By means of the second equation in (48) we can derive the fluxes. We have

$$\mathfrak{F}_j = \sum_{k=j+1}^{r} a_{jk}\mathfrak{F}_k + a_j\mathfrak{S}_r - 4\{A_j e^{\lambda_j t} - B_j e^{-\lambda_j t}\} . \tag{53}$$

We have now to introduce the boundary conditions. Let t_1 be the value of t at the outer boundary of the nebula. Then we have the well-known conditions for a planetary nebula:

$$\mathfrak{F}_j = 0 \qquad \text{when} \qquad t = 0 ,$$
$$\mathfrak{F}_j = 2\mathfrak{J}_j \qquad \text{when} \qquad t = t_1 .$$

The first condition gives

$$A_j - B_j = \frac{a_j}{4}\mathfrak{S}_r^0 ,$$

while the second gives

$$\tfrac{1}{2}\sum_{k=j+1}^{r} a_{jk}\left(\frac{\mu_j}{\mu_k} - 1\right)\mathfrak{F}_k(t_1) + \tfrac{1}{4}a_j\left(\frac{3\mu_j}{\mu_r} - 2\right)\mathfrak{S}_r(t_1)$$
$$+ A_j\left(\frac{3\mu_j}{\lambda_j} + 2\right)e^{\lambda_j t_1} + B_j\left(\frac{3\mu_j}{\lambda_j} - 2\right)e^{-\lambda_j t} = 0 .$$

Solving for the constants, we find that

$$A_j = \frac{1}{4}\,\frac{a_j\mathfrak{S}_r^0\left(\frac{3\mu_j}{\lambda_j} - 2\right)e^{-\lambda_j t_1} - 2\sum_{k=j+1}^{r} a_{jk}\left(\frac{\mu_j}{\mu_k} - 1\right)\mathfrak{F}_k(t_1) - a_j\left(\frac{3\mu_j}{\mu_r} - 2\right)\mathfrak{S}_r(t_1)}{\left(\frac{3\mu_j}{\lambda_j} + 2\right)e^{\lambda_j t_1} + \left(\frac{3\mu_j}{\lambda_j} - 2\right)e^{-\lambda_j t_1}} ,$$

$$B_j = -\frac{1}{4}\,\frac{a_j\mathfrak{S}_r^0\left(\frac{3\mu_j}{\lambda_j} + 2\right)e^{\lambda_j t_1} + 2\sum_{k=j+1}^{r} a_{jk}\left(\frac{\mu_j}{\mu_k} - 1\right)\mathfrak{F}_k(t_1) + a_j\left(\frac{3\mu_j}{\mu_r} - 2\right)\mathfrak{S}_r(t_1)}{\left(\frac{3\mu_j}{\lambda_j} + 2\right)e^{\lambda_j t_1} + \left(\frac{3\mu_j}{\lambda_j} - 2\right)e^{-\lambda_j t_1}} .$$

The emergent flux becomes, after substituting the values of the constants,

$$\left.\begin{aligned}\mathfrak{F}_j(t_1) = \sum_{k=j+1}^{r} a_{jk}\mathfrak{F}_k(t_1)\,\frac{\frac{3}{\lambda_j}\cosh\lambda_j t_1 + \frac{2}{\mu_k}\sinh\lambda_j t_1}{\frac{3}{\lambda_j}\cosh\lambda_j t_1 + \frac{2}{\mu_j}\sinh\lambda_j t_1} \\ + 3a_j\mathcal{S}_r^0 e^{-\mu_r t_1}\,\frac{\frac{1}{\lambda_j}\cosh\lambda_j t_1 + \frac{1}{\mu_r}\sinh\lambda_j t_1 - \frac{1}{\lambda_j}e^{\mu_r t_1}}{\frac{3}{\lambda_j}\cosh\lambda_j t_1 + \frac{2}{\mu_j}\sinh\lambda_j t_1}\,.\end{aligned}\right\} \quad (54)$$

When $j = 2$, $\beta_{22} = p_{21} = 1$ and $\lambda_2 = 0$. From (43), (51), and (52)

$$a_{2k} = -1\,, \qquad a_2 = -1\,.$$

Equation (54) becomes

$$\mathfrak{F}_2(t_1) = -\sum_{k=3}^{r}\mathfrak{F}_k(t_1) + \mathcal{S}_r^0(1 - e^{-\mu_r t_1})\,,$$

which also follows from the flux integral.

We are now in a position to determine the intensities for transitions not involving the ground state. The emission coefficient $\mathcal{B}_{ij}N_j$ is, by (46),

$$N_1\sum_{k=j}^{r}\beta_{kji}\mu_k(\mathcal{J}_k + \tfrac{1}{4}\mathcal{S}_k)\,,$$

where we have written

$$\beta_{kji} = q_{kj}p_{ji} = \beta_{kj}\frac{p_{ji}}{p_{j1}}\,. \quad (55)$$

The absorption coefficient

$$\mu_{ij}(N_i - N_j)$$

is a linear combination of intensities and is consequently a small quantity. When it is multiplied by an intensity, as it is in the equa-

tion of transfer, we get a term which can be neglected in comparison with the emission term. Consequently,

$$\frac{d\mathfrak{F}_{ij}}{dt} = 4\sum_{k=j}^{r} \beta_{kji}\mu_k \mathfrak{J}_k + \beta_{rji}\mu_r \mathfrak{S}_r \,. \tag{56}$$

Now, equation (48) shows that

$$\frac{d\mathfrak{F}_j}{dt} = 4\sum_{k=j}^{r} \beta_{kj}\mu_k \mathfrak{J}_k + \beta_{rj}\mu_r \mathfrak{S}_r - 4\mu_j \mathfrak{J}_j \,.$$

It is possible to solve these equations for $\mathfrak{J}_k$. We suppose that

$$\mu_k \mathfrak{J}_k = -\tfrac{1}{4}\sum_{l=k}^{r} \tilde{\omega}_{kl} \frac{d\mathfrak{F}_l}{dt} + \tfrac{1}{4}\tilde{\omega}_k \mu_r \mathfrak{S}_r \,. \tag{57}$$

To determine the coefficients, introduce this into the previous equation:

$$\frac{d\mathfrak{F}_j}{dt} = -\sum_{k=j}^{r} \beta_{kj} \left\{ \sum_{l=k}^{r} \tilde{\omega}_{kl} \frac{d\mathfrak{F}_l}{dt} - \tilde{\omega}_k \mu_r \mathfrak{S}_r \right\} + \beta_{rj}\mu_r \mathfrak{S}_r + \sum_{l=j}^{r} \tilde{\omega}_{jl} \frac{d\mathfrak{F}_l}{dt} - \tilde{\omega}_j \mu_r \mathfrak{S}_r \,,$$

$$= \sum_{l=j}^{r} \frac{d\mathfrak{F}_l}{dt} \left\{ \tilde{\omega}_{jl} - \sum_{k=j}^{l} \beta_{kj}\tilde{\omega}_{kl} \right\} + \mu_r \mathfrak{S}_r \left\{ \beta_{rj} - \tilde{\omega}_j + \sum_{k=j}^{r} \beta_{kj}\tilde{\omega}_k \right\} .$$

Therefore,

$$1 = \tilde{\omega}_{jj} - \beta_{jj}\tilde{\omega}_{jj} \,,$$

$$0 = \tilde{\omega}_{jl} - \sum_{k=j}^{l} \beta_{kj}\tilde{\omega}_{kl} \,, \qquad (l > j)$$

$$0 = \beta_{rj} - \tilde{\omega}_j + \sum_{k=j}^{r} \beta_{kj}\tilde{\omega}_k \,.$$

From these follow the equations:

$$\tilde{\omega}_{jj} = \frac{1}{1 - \beta_{jj}}, \qquad \tilde{\omega}_{jl} = \frac{\sum_{k=j+1}^{l} \beta_{kj}\tilde{\omega}_{kl}}{1 - \beta_{jj}}, \qquad \tilde{\omega}_{j} = \frac{\beta_{rj} - \sum_{k=j+1}^{r} \beta_{kj}\tilde{\omega}_{k}}{1 - \beta_{jj}}. \quad (58)$$

Equation (57) can now be introduced into (56) and the integration performed. The result is

$$\mathcal{F}_{ij} = -\sum_{k=j}^{r}\sum_{l=k}^{r} \beta_{kji}\tilde{\omega}_{kl}\mathcal{F}_{l} + (\mathcal{S}_{r}^{0} - \mathcal{S}_{r})\left(\beta_{rji} + \sum_{k=j}^{r} \beta_{kji}\tilde{\omega}_{k}\right).$$

Using (55) and (58), we can write this in a slightly different form:

$$\mathcal{F}_{ij} = \frac{p_{ji}}{p_{j1}}\left\{\mathcal{F}_{j} - \sum_{l=j}^{r} \tilde{\omega}_{jl}\mathcal{F}_{l} + \tilde{\omega}_{j}\mathcal{S}_{r}^{0}(1 - e^{-\mu_{r}t_{1}})\right\}, \qquad (59)$$

where we have substituted for β_{jj} its value p_{j1}. Here we have utilized the vanishing of the fluxes on the inner surface of a planetary nebula.

As an alternative procedure for these transitions we could have considered the specific intensity directly. For the equation of transfer we have

$$\cos\theta \frac{d\mathcal{I}_{ij}}{dt} = \sum_{k=j}^{r} \beta_{kji}\mu_{1k}(\mathcal{I}_{k} + \tfrac{1}{4}\mathcal{S}_{k}).$$

Since the right-hand side is a function only of t, we can integrate this equation as it stands. Evidently the intensity will be proportional to sec θ, so that it will increase very rapidly with increasing values of the angle of observation. The actual infinite value of the intensity must not be taken seriously, since it is due to the approximations involved—the neglect of absorption effects and the representation of the nebula as a plane-parallel sheet. Struve[7] has found that in certain diffuse nebulae the conditions necessary for the existence of the effect are satisfied. His explanation is essentially the same as that given here.

[7] *Ap. J.*, **85**, 194, 1937.

This completes the formal development of the theory for a set of discrete states. The remaining steps are those necessary to generalize the equations to the continuum.

THE CONTINUUM

Ambarzumian[8] has shown that the continuum can be treated approximately as a discrete state, provided the weight is chosen appropriately. More recently Menzel and Pekeris[9] have shown that each element of the continuum can be treated as a discrete state, when the weight of the element is taken according to the formula of Fowler. Now the number of atomic systems in velocity range $(v, v + dv)$ for the free electrons is

$$n_i f(v) dv ,$$

where n_i is the number of ionized atoms in unit volume and $f(v)$ represents the distribution of velocities. The statistical weight of this element is

$$\frac{8\pi m^3 v^2 dv}{n_e h^3} ,$$

where n_e is the number of free electrons in unit volume. Hence, the number of systems per unit volume per unit weight is

$$\dot{N}(v) = \frac{h^3}{8\pi m^3} \frac{n_i n_e f(v)}{v^2} .$$

Without additional comment it is evident that the equation of transfer for the ith continuum can be put in the form (cf. [10], [11], and [12])

$$\frac{d\mathcal{J}_i(\nu)}{dt} = \mathcal{B}_i(\nu) N(\nu) + \{N(\nu) - N_i\} \mu_i(\nu) \mathcal{J}_i(\nu) , \qquad (12')$$

where the upper state is denoted by the frequency corresponding to the electron velocity, that is

$$\nu = \frac{mv^2}{2h} .$$

[8] *Op. cit.* [9] *M.N.*, **96**, 77, 1935.

In (12′), $\mathcal{J}_i(\nu)$ represents the photon intensity in unit frequency intervals. It must be emphasized that the quantities $\mathcal{B}_i(\nu)$ and $\mu_i(\nu)$ are atomic functions and consequently do not vary from point to point in the nebula.

Strictly speaking, (12′) gives only the partial variation of the intensity due to transitions between the states indicated. In general, the various continua overlap each other and the continuum formed by free-free transitions. Actually the effect of this overlapping is quite small for the first continuum and is purely formal for the others, since for $i > 1$ (and for free-free transitions) the second term on the right-hand side of (12′) can be neglected, as we shall see, removing all coupling between the different types of transitions. For the present, however, we shall regard (12′) as giving the net exchange between the two states.

Similarly,

$$\frac{d\mathcal{J}(\nu, \nu')}{ds} = \mathcal{B}(\nu, \nu')N(\nu') + \{N(\nu') - N(\nu)\}\mu(\nu, \nu')\mathcal{J}(\nu, \nu') \quad (12'')$$

gives the partial variation of the intensity due to free-free transitions, or the net exchange of systems between the states ν and ν'.

The complete set of equations representing the condition of radiative equilibrium is as follows (cf. [14]):

$$\left.\begin{aligned}
&\sum_{j=1}^{i-1}\{N_i\mathcal{B}_{ji} + (N_i - N_j)\mu_{ji}\mathcal{J}_{ji}\} - \sum_{j=i+1}^{\infty}\{N_j\mathcal{B}_{ij} + (N_j - N_i)\mu_{ij}\mathcal{J}_{ij}\} \\
&\qquad - \int_0^{\infty}\{N(\nu')\mathcal{B}_i(\nu') + [N(\nu') - N_i]\mu_i(\nu')\mathcal{J}_i(\nu')\}d\nu' = 0, \\
&\sum_{j=1}^{\infty}\{N(\nu)\mathcal{B}_j(\nu) + [N(\nu) - N_j]\mu_j(\nu)\mathcal{J}_j(\nu)\} \\
&\quad + \int_0^{\nu}\{N(\nu)\mathcal{B}(\nu', \nu) + [N(\nu) - N(\nu')]\mu(\nu', \nu)\mathcal{J}(\nu', \nu)\}d\nu' \\
&- \int_{\nu}^{\infty}\{N(\nu')\mathcal{B}(\nu, \nu') + [N(\nu') - N(\nu)]\mu(\nu, \nu')\mathcal{J}(\nu, \nu')\}d\nu' = 0.
\end{aligned}\right\} \quad (14')$$

For dilute radiation the solution of these equations is the generalization of (36) or of (44).

If we define the quantities $p(\nu)_i$ and $p(\nu, \nu')$ by the equations

$$\left.\begin{aligned} p(\nu)_i &= \frac{\mathcal{B}_i(\nu)}{\sum_{k=1}^{\infty}\mathcal{B}_k(\nu) + \int_0^{\nu}\mathcal{B}(\nu', \nu)d\nu'}, \\ p(\nu, \nu') &= \frac{\mathcal{B}(\nu', \nu)}{\sum_{k=1}^{\infty}\mathcal{B}_k(\nu) + \int_0^{\infty}\mathcal{B}(\nu'', \nu)d\nu''}, \end{aligned}\right\} \tag{41'}$$

and $q(\nu)_i$ and $q(\nu, \nu')$ by

$$\left.\begin{aligned} q(\nu)_i &= p(\nu)_i + \sum_{k=i+1}^{\infty} q(\nu)_k p_{ki} + \int_0^{\nu} q(\nu, \nu')p(\nu')_i d\nu', \\ q(\nu, \nu') &= p(\nu, \nu') + \int_{\nu'}^{\nu} q(\nu, \nu'')p(\nu'', \nu')d\nu'', \end{aligned}\right\} \tag{43'}$$

the generalization of (44) is

$$\left.\begin{aligned} \frac{N_j}{N_1}\sum_{k=1}^{j-1}\mathcal{B}_{kj} &= \mu_{1j}\mathcal{J}_{1j} + \sum_{l=j+1}^{\infty} q_{lj}\mu_{1l}\mathcal{J}_{1l} + \int_0^{\infty} q(\nu')_j\mu_1(\nu')\mathcal{J}_1(\nu')d\nu', \\ \frac{N(\nu)}{N_1}\left\{\sum_{k=1}^{\infty}\mathcal{B}_k(\nu) + \int_0^{\nu}\mathcal{B}(\nu', \nu)d\nu'\right\} &= \mu_1(\nu)\mathcal{J}_1(\nu) \\ &\quad + \int_{\nu}^{\infty} q(\nu', \nu)\mu_1(\nu')\mathcal{J}_1(\nu')d\nu'. \end{aligned}\right\} \tag{44'}$$

Equations (44′) follow from the same line of reasoning that we employed in deriving (44), and therefore depend on the assumption of the high dilution of the incident radiation. Furthermore, (44′) justifies our deductions concerning the effect of overlapping.

Hence, in the case of stratification in parallel planes, (14′) leads to the generalized flux integrals

$$\left.\begin{aligned} \sum_{j=1}^{i-1}\mathcal{F}_{ji} - \sum_{j=i+1}^{\infty}\mathcal{F}_{ij} - \int_0^{\infty}\mathcal{F}_i(\nu)d\nu &= a_i, \\ \sum_{j=1}^{\infty}\mathcal{F}_j(\nu) + \int_0^{\nu}\mathcal{F}(\nu', \nu)d\nu' - \int_{\nu}^{\infty}\mathcal{F}(\nu, \nu')d\nu' &= a(\nu) \end{aligned}\right\} \tag{18'}$$

It should be remembered that the continuous fluxes in (18′) have a meaning only if we are able to separate the component continua in the blended spectrum. Without any difficulty it can also be shown that (18′) leads to the generalized K-integral

$$\left.\begin{aligned}\sum_{i=1}^{\infty}\left\{\sum_{j=i+1}^{\infty}\frac{\mathcal{K}_{ij}-\frac{1}{4}\mathcal{F}_{ij}^{0}\tau_{ij}}{\mu_{ij}}+\int_{0}^{\infty}\frac{\mathcal{K}_{i}(\nu)-\frac{1}{4}\mathcal{F}_{i}^{0}(\nu)\tau_{i}(\nu)}{\mu_{i}(\nu)}\,d\nu\right\}\\ +\int_{0}^{\infty}\int_{\nu}^{\infty}\frac{\mathcal{K}(\nu,\nu')-\frac{1}{4}\mathcal{F}^{0}(\nu,\nu')\,\tau\,(\nu,\nu')}{\mu(\nu,\nu')}\,d\nu'd\nu=0.\end{aligned}\right\}\quad(29')$$

Finally, we remark that the generalization of the τ-integrals is trivial and need not be considered further.

The equations (44′) being available, it is possible to proceed along the lines followed in the preceding section in solving the differential equations of the radiation field. It is evident that the formal exposition will differ in no way from that followed in the discrete case, and we shall arrive at generalizations of (50), (51), (52), (53), and (54), in which the summations have been extended to integration over the continuous states. In particular, (51) and (52) become the pair of equations

$$a_j(\nu)=\frac{3\mu(\nu)^2}{\lambda_j^2-\lambda(\nu)^2}\left\{\beta(\nu)_j-\sum_{l=j+1}^{\infty}a_{jl}\beta(\nu)_l-\int_{0}^{\nu}a_j(\nu')\beta(\nu,\nu')d\nu'\right\},\quad(51')$$

$$a(\nu,\nu')=\frac{3\mu(\nu')^2}{\lambda(\nu)^2-\lambda(\nu')^2}\left\{\beta(\nu',\nu)-\int_{\nu}^{\nu'}a(\nu,\nu'')\beta(\nu',\nu'')d\nu''\right\},\quad(52')$$

of which the second is an integral equation. In addition, $\beta(\nu,\nu')$ depends on the solution of the integral equation in (43′). The discussion of these integral equations is beyond the scope of the present investigation, and we shall leave the problem in its present stage. The general solution of the continuous problem is under consideration and will be reported in a future communication.

FOUR-STATE PROBLEM

We close our discussion with a consideration of the four-state problem for a planetary nebula. From (43) we have

$$q_{43}=p_{43},\qquad q_{42}=p_{42}+p_{43}p_{32},\qquad q_{32}=p_{32};$$

also

$$\beta_{44} = p_{41}\,, \quad \beta_{43} = p_{43}p_{31}\,, \quad \beta_{42} = p_{42} + p_{43}p_{32}\,, \quad \beta_{33} = p_3\,,$$

$$\beta_{32} = p_{32}\,, \quad \beta_{22} = 1\,.$$

From the definition of λ_j, we have

$$\lambda_4^2 = 3\mu_4^2(1 - p_{41})\,, \qquad \lambda_3^2 = 3\mu_3(1 - p_{31})\,, \qquad \lambda_2^2 = 0\,.$$

Furthermore, from (51) we have

$$a_{34} = \frac{p_{43}p_{31}}{\left(\frac{\mu_3}{\mu_4}\right)^2(1 - p_{31}) - (1 - p_{41})}\,, \qquad a_{23} = -1\,, \qquad a_{24} = -1\,,$$

and from (52)

$$a_4 = \frac{p_{41}}{2 - 3p_{41}}\,, \qquad a_3 = \frac{p_{43}p_{31} - a_{34}p_{41}}{3\left(\frac{\mu_3}{\mu_4}\right)^2(1 - p_{31}) - 1}\,, \qquad a_2 = -1\,.$$

If we associate the fourth state with the continuum, the quantity μ_3/μ_4 will be a large quantity of the order of 10^4. Taking this value, we have

$$a_{34} \sim 10^{-8}\,\frac{p_{43}p_{31}}{p_{32}}\,, \qquad a_3 \sim \tfrac{1}{3}\,10^{-8}\,\frac{p_{43}p_{31}}{p_{32}}\,.$$

From (54)

$$\mathcal{J}_4(t_1) \doteq \frac{3p_{41}}{2 - 3p_{41}}\,\mathcal{S}_4^0 e^{-\mu_4 t_1}\,\frac{\cosh\lambda_4 t_1 + \frac{\lambda_4}{\mu_4}\sinh\lambda_4 t_1 - e^{\mu_4 t_1}}{3\cosh\lambda_4 t_1 + \frac{2\lambda_4}{3\mu_4}\sinh\lambda_4 t_1}$$

and

$$\mathcal{J}_3(t_1) = \frac{2\times 10^{-8}}{\mu_4}\,\frac{p_{43}p_{31}}{p_{32}}\,\frac{\sinh\lambda_3 t_1 \mathcal{J}_4(t_1)}{\frac{3}{\lambda_3}\cosh\lambda_3 t_1 + \frac{2}{\mu_3}\sinh\lambda_3 t_1}$$

$$+ \frac{10^{-8}}{\mu_4}\,\frac{p_{43}p_{31}}{p_{32}}\,\mathcal{S}_4^0 e^{-\mu_4 t_1}\,\frac{\sinh\lambda_3 t_1}{\frac{3}{\lambda_3}\cosh\lambda_3 t_1 + \frac{2}{\mu_3}\sinh\lambda_3 t_1}\,,$$

where we have made use of the fact that λ_3/λ_4 is large. Now, except for small values of $\lambda_4 t_1$, the optical thickness in the continuum, this becomes

$$\mathcal{F}_3(t_1) = 2 \times 10^{-4} \frac{p_{43}p_{31}}{p_{32}} \frac{\lambda_3}{3\mu_3 + 2\lambda_3} \{\mathcal{F}_4(t_1) + \tfrac{1}{2}\mathcal{S}_4^0\} e^{-\mu_4 t_1},$$

which is a small quantity. Finally,

$$\mathcal{F}_2(t_1) = \mathcal{S}_4^0(1 - e^{-\mu_4 t_1}) - \mathcal{F}_3(t_1) - \mathcal{F}_4(t_1) \sim \mathcal{S}_4^0(1 - e^{-\mu_4 t_1}) - \mathcal{F}_4(t_1).$$

Now we have

$$\tilde{\omega}_{44} = \frac{1}{1 - p_{41}}, \qquad \tilde{\omega}_4 = \frac{p_{41}}{1 - p_{41}}, \qquad \tilde{\omega}_{34} = \frac{p_{43}p_{31}}{p_{32}(1 - p_{41})}.$$

Hence,

$$\frac{1}{p_{43}}\mathcal{F}_{34} = \frac{1}{p_{42}}\mathcal{F}_{24} = \frac{1}{p_{43}}\mathcal{F}_{23} = \frac{1}{1 - p_{41}}\{\mathcal{S}_4^0(1 - e^{-\mu_4 t_1}) - \mathcal{F}_4\}.$$

In Figures 1–4 are shown the curves for the various fluxes as functions of $\mu_4 t_1 = \tau$. Various combinations of the p_{ji} have been used in computing these. Perhaps the most striking feature is the weakness of $\mathcal{F}_3$, which is roughly one ten-thousandth of the other intensities. This is certainly independent of the fact that we have considered only four states, and it will be true in a more general discussion. Hence, we are led to the fact that the Lyman series, excepting Ly α, is much weaker than the other hydrogen series. The features of the curves for $\mathcal{F}_{14}$ and $\mathcal{F}_{12}$ are, of course, identical with those of Chandrasekhar.[10]

YERKES OBSERVATORY
March 1938

[10] *Op. cit.*

SODIUM IN THE UPPER ATMOSPHERE

J. CABANNES, J. DUFAY, AND J. GAUZIT

ABSTRACT

Spectroscopic and interferometer observations show conclusively that the bright yellow radiation of the night sky coincides with the two D lines and that sodium atoms are always present in the upper atmosphere. At twilight the yellow radiation is increased, like the red line λ 6300 of [*O* I]. The writers are examining the altitude of the luminescent layer and the origin of atmospheric sodium; they believe that the sodium comes from meteorites.

I. THE YELLOW RADIATION OF THE NIGHT SKY AND ITS ATMOSPHERIC ORIGIN

Among the lines or bands discovered by Slipher[1] in the spectrum of the night sky, the bright yellow radiation near the sodium D lines calls for special attention.

While the green line λ 5577 and the red doublet λλ 6300–6364 have for several years been definitely identified with the lines $^1S_0 \rightarrow {}^1D_2$ and $^1D_2 \rightarrow {}^3P_{2,1}$, of the oxygen atom [*O* I], the origin of the yellow radiation was still unknown a few months ago.

The results of wave-length measurements taken by several observers are summarized as follows:

		Angstrom Units
V. M. Slipher*	1929	5892
J. Dufay†	1932	5892.5
L. A. Sommer‡	1932	5888
J. Cabannes§	1934	5888
L. Vegard and E. Tønsberg‖	1935	5885

* *Pub. A.S.P.*, **41**, 263, 1929.
† *C.R.*, **194**, 1897, 1932; *J. de Phys.*, **4**, 221, 1933.
‡ *Zs. f. Phys.*, **77**, 374, 1935.
§ *J. de Phys.*, **5**, 601, 1934.
‖ *Zs. f. Phys.*, **94**, 413, 1935.

The great discrepancies between these results have prevented earlier attempts to identify this line. New measurements were made on numerous plates obtained at Montpellier[2] in 1935, 1936, and 1937, using the Cojan spectrograph with large aperture, f/0.7. This spectrograph gives excellent reproductions of the yellow line at

[1] *Pub. A.S.P.*, **41**, 263, 1929.
[2] *C.R.*, **206**, 221, 1938.

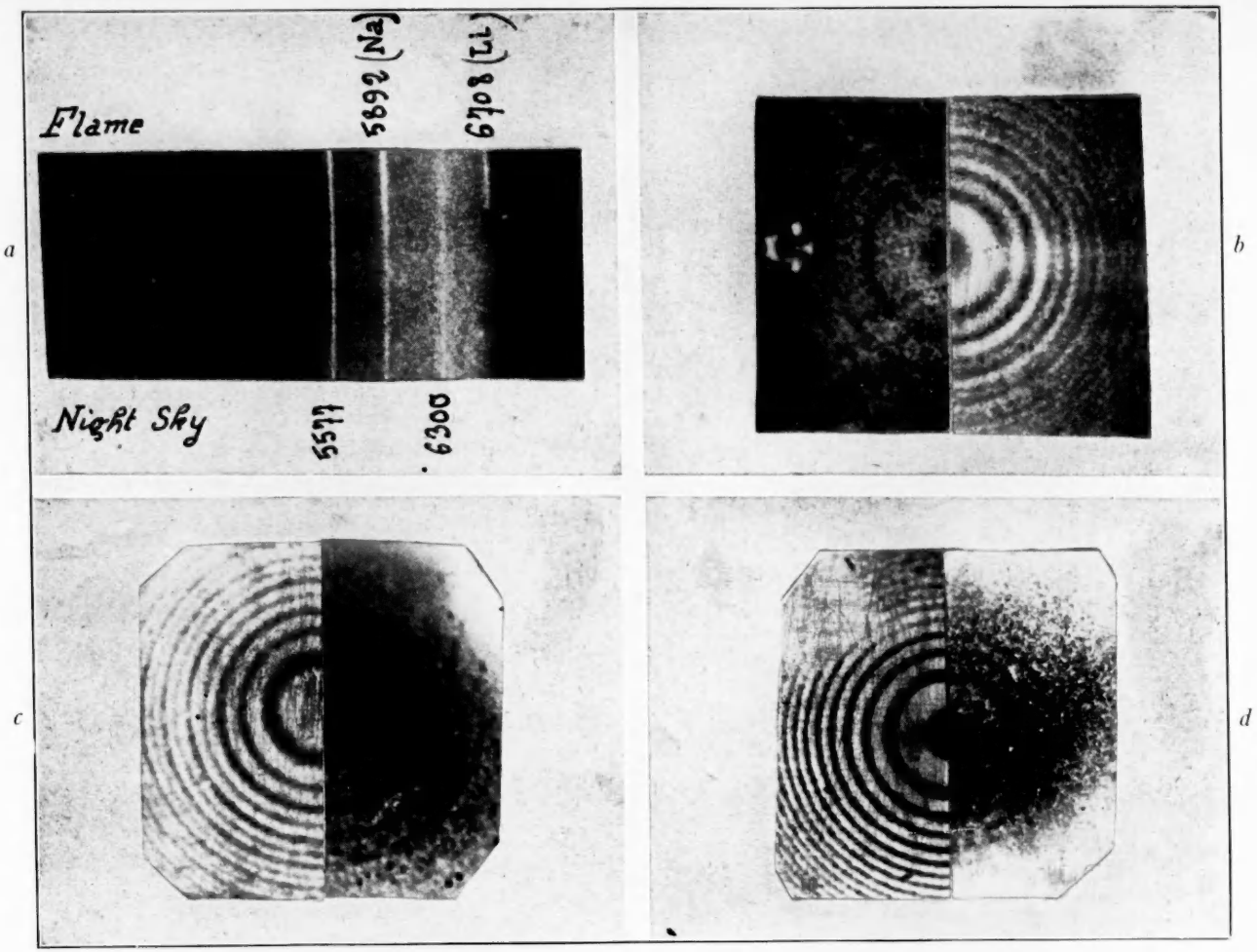

a) The spectrum of the night sky at Montpellier, France

b) Fringes obtained at night with 0.15-mm étalon: on the right, sodium fringes; on the left, fringes of the night sky (Lyon Observatory)

c) Fringes obtained at twilight with 0.15-mm étalon: on the left, sodium; on the right, twilight (Lyon Observatory)

d) Fringes obtained at twilight with 0.30-mm étalon: on the left, sodium; on the right, twilight (Lyon Observatory)

twilight or at night, with half-hour exposures. Panchromatic "Ilford Hypersensitive" plates and Eastman F, Type I, plates were successfully used. Near λ 5900 the dispersion is about 500 A per millimeter. The width of the yellow radiation, on the plates, is 20 μ; errors arising from the measurements of its center of gravity do not seem to exceed about ± 1 μ.

The average value of the measurements taken on the ten best plates is λ 5894 ± 1 A. The yellow radiation of the night sky is therefore certainly quite close to the D lines.

On the photograph reproduced here (Pl. VI*a*), part of the slit was illuminated by a sodium flame. The two D lines, which are not resolved by the spectrograph, have the same appearance as the sky radiation and are found in its continuation; however, they are perhaps displaced by 1 or 2 A toward the shorter wave lengths.

In addition, the yellow radiation in our spectrograms has the same appearance as the D system and differs from the line λ 5577; the intensity of the yellow radiation decreases gradually on each side of the maximum, while in the case of the λ 5577 line the intensity decreases abruptly. The λ 5894 line of the sky seems, therefore, to be a complex radiation.

A microphotometer tracing of the spectrum (the microphotometer enlarges seventy times) shows that the width of the line λ 5894, measured at mid-height, is greater than the widths of the lines λ5577 and λ 6300; the presence, on either side of λ 5896, of two lines a few angstroms away explains clearly this difference. The yellow radiation of the sky and the unresolved sodium D lines give similar diagrams.

Observations by Dufay in 1932 were made by means of a fine wire set in the middle of a wide slit. The shadow of the wire was always narrower and less clear in the yellow image than in the image of the green line λ 5577. This fact also seems to prove the complexity of the yellow radiation.

Dufay examined, in 1932, the possibility of emission by interstellar sodium atoms; but the difference in intensity at the zenith and near the horizon and, in particular, the variations in intensity from night to night and during the same night gave evidence that the radiation was emitted in the upper atmosphere. Furthermore,

b) Fringes obtained at twilight with 0.15-mm étalon: on the left, sodium; on the right, twilight (Lyon Observatory)
c) Fringes obtained at twilight with 0.15-mm étalon: on the left, sodium; on the right, twilight (Lyon Observatory)

a long series of observations made by Garrigue at the Pic-du-Midi[3] put the atmospheric origin of the yellow radiation of the night sky beyond all doubt: the intensity of the radiation becomes two or three times greater from the zenith to the horizon. In addition, although the yellow radiation does not undergo regular variations during the night, as does the green line λ 5577 A, it seems to show fairly well-marked annual variations, the maximum occurring during the winter and the minimum in the summer.

The hypothesis of an emission of sodium in the upper atmosphere, however strange it may appear to be, cannot be neglected.

II. INTERFEROMETER ANALYSIS OF THE YELLOW RADIATION AT NIGHT

The verification of this hypothesis requires the use of an apparatus able to resolve the two D lines. Since the spectrographs which we are using at the present moment have great light-gathering power but are of low dispersion and are not capable of separating the D lines, we have tried to analyze the structure of the radiation of the night sky with the help of an interferometer, which is easier to construct and is less costly than a prismatic apparatus.

With a Fabry-Perot interferometer with air blades between half-silvered surfaces, the fringes to infinity resulting from the D_1 radiation insert themselves exactly between the fringes resulting from the D_2 radiation, when the thickness of the air blade is 0.15 mm. When the thickness is 0.30 mm, the two systems of fringes are, on the contrary, superposed. Working alternatively with these two thicknesses, we can, therefore, detect whether the yellow radiation of the night sky has the same structure as the D lines.

The Fabry-Perot interferometers were composed of two plane-parallel glasses lightly silvered on one side and separated by three pieces of metallic wire. Invar wires 0.15 mm in thickness and platinum wires 0.30 mm in thickness were used.

The first method.—In the first series of experiments the interferometer was adjusted in front of a small two-prism spectrograph the camera lens of which has a relative aperture f/1 and a focal length of 25 mm. A lens of 6 or 10 cm focal length projects the fringes on

[3] *Ibid.*, **202**, 1807, 1936; **205**, 491, 1937.

the slit. With exposures of 20 hours or more, we have observed distinctly, with the 0.15 mm interferometer, very crowded rings in the yellow radiation. The aspect of these fringes was exactly the same as that of the fringes given by the two D lines. At the same time, the fringes of the λ 5577 and λ 6300 lines of [*O* I] were intense. Agfa *ISS* panchromatic plates, hypersensitized before use in a diluted solution of ammonia, were used. The first positive result was obtained with a 27-hour exposure from February 28 to March 4, 1938.[4]

The second method.—The intensity of the yellow radiation makes it possible to obtain interference fringes without the use of a spectrograph, provided the λ 5577 and λ 6300 lines are eliminated. An orange filter (Schott glass OG2, 2 or 4 mm thick) can be used to absorb the green line. In order to be free from the red line, it is necessary to use plates whose sensitivity is weak at λ 6300. Crumière Panchro P plates fulfil this condition.

We have photographed in this manner interference fringes at night with the Fabry-Perot etalon placed in front of a camera lens of 25 mm focal length and a relative aperture f/1. Using alternatively thicknesses of 0.30 and 0.15 mm, one or two systems of fringes appeared. The fringes are several millimeters in diameter and can be accurately measured. In every case their diameters differed by almost 0.01 mm from the diameters of the sodium fringes photographed on the same plate. The D_2 fringes are, as in the laboratory, about twice as intense as the D_1 fringes. Plate VI*b* shows the enlargement of a plate obtained from March 30 to April 2, 1938 (exposure 22 hours), with the 0.15 mm etalon. The copies of the fringes were cut along a diameter. We see that the fringes of the night-sky radiation are an exact continuation of those of the sodium flame. The sharpness of the outline, however, has been increased in the reproduction, and the former D_1 fringes are nearly indistinguishable on the sky photograph. One night's exposure is sufficient to give distinct but faint fringes; clear photographs require two or three nights' exposures.

The preceding observations prove conclusively that the yellow radiation of the night sky is contained in the two D *lines and that sodium atoms are always present in the upper atmosphere.*

[4] *Ibid.*, **206**, 870, 1938.

III. THE YELLOW RADIATION AT TWILIGHT AND ITS INTERFEROMETER ANALYSIS

During the International Polar Year, 1932–1933, B. W. Currie and H. W. Edwards observed spectra of the polar aurora and of the night sky at Chesterfield, Keewatin, Canada.[5] They found that the intensities of the yellow radiation and of the red line λ 6300 were increased during twilight.[6] However, their paper appeared only in 1936, and the strong excitation of the λ 6300 line had been already discovered and carefully studied by Cabannes and Garrigue at the Pic-du-Midi.[7]

The excitation of the yellow radiation was found again and studied by Bernard at Tromsø in 1937.[8] From his photometric measures it appears that the luminescence ends abruptly when the solar rays tangent to the earth reach an altitude of about 60 km. According to Bernard, there is a thin luminescent layer at this altitude, and the yellow radiation is excited by optical resonance.

The interferometer analysis of the yellow radiation at twilight is much easier than at night, because of its stronger intensity. We have carried out the same experiments at twilight as at night. By our first method we photographed, with the spectrograph, fringes quite similar to the sodium fringes, with thicknesses of 0.15 and 0.30 mm in the interferometer. Exposures of 10–20 minutes are now sufficient. By the second method we regularly photographed interference fringes with exposures of 20–35 minutes. The exposures began in the evening when the sun was about 8° below the horizon. The camera was pointed toward the west, 10° or 20° high. In the morning the camera was pointed toward the east and the exposure was closed

[5] *Terrestrial Magnetism*, **41**, 265, 1936.

[6] In a recent paper (*C.R.*, **206**, 1137, 1938) R. Bernard attempts to show that the observations of B. W. Currie and H. W. Edwards did not concern the λ 5893 radiation. The wave length measured by Currie and Edwards was, indeed, λ 5940; but their measurements were not precise and they concluded that "this radiation is due to a luminescence distinct from that of the aurora and is probably the radiation of 5893 A observed by Vegard and Tønsberg in the night sky." Therefore, Bernard's argumentation does not seem to us convincing. According to Currie and Edwards, the intensity of the yellow radiation is also increased during periods of moonlight.

[7] *Ibid.*, **202**, 1807, 1936; **203**, 484, 1936.

[8] *Ibid.*, **206**, 448, 1938.

when the sun reached the same altitude. The fringes were also photographed at the zenith, later in the morning and earlier in the evening, with a 15-minute exposure.

Plate VI*c* and *d* shows enlargements of plates made at twilight with the interferometer 0.15 and 0.30 mm thick. The identity in appearance with the sodium fringes is very noticeable; and, in the case of the 0.15-mm thickness, the intensity ratio of the two components seems to be the same in the sky as in the laboratory.

At the same time, Bernard published quite similar results obtained during twilight, following the second method.[9]

In the conclusion of this article we shall deal only with the emission of the yellow sodium radiation during the night.

IV. RELATIVE INTENSITIES OF THE TWO COMPONENTS OF THE DOUBLET

Our first measurements placed the center of gravity of the doublet at 5894 ± 1 A. We concluded from this that in the night sky the two components D_1 and D_2 had the same intensity (as is the case in the spectra of comets[10]). The interferometer studies have not confirmed this result: Plate VI*b* shows that component D_1 gives fainter rings than D_2; the intensity ratio is near the theoretical ratio 1/2.

V. ALTITUDE OF THE LUMINESCENT LAYER

The observations made by Garrigue at the Pic-du-Midi in December, 1935, and January, 1936, give B_H/B_z as the ratio between the intensity of the yellow radiation at the horizon and at the zenith. The average of the intensities, which are very close to each other, as measured by Garrigue in the different azimuths at about 10° above the horizon, is 2.8 times greater than the intensity at the zenith. From this number we may derive the altitude of the luminescent layer, supposedly homogeneous and relatively thin. When we observe one point in the sky, the apparent brightness is the sum of a term TB_0, which gives the real brightness B_0 of the sky at that particular point, reduced by atmospheric absorption, and a term B',

[9] *Ibid.*, p. 928, 1938.

[10] A. Adel, V. M. Slipher, and R. Ladenburg, *Ap. J.*, **86**, 345, 1937.

which is the result of the scattering by the lower atmosphere, for the whole length of the visual ray, of the light given out by the entire sky. The equation

$$B = TB_0 + B'$$

may be applied to the following four cases: the monochromatic luminescence of the sodium layer at 10° above the horizon and at the zenith, the scattering of the light of the stars by the interstellar particles, following the same directions.

The observation of the continuous spectrum of the night sky gives

$$\frac{B_H}{B_z} = \frac{T_H + \frac{B'_H}{B_0}}{T_z + \frac{B'_z}{B_0}} = 0.86 . \qquad (1)$$

An a priori calculation[11] shows fairly exactly the light diffused along a vertical ray:

$$\frac{B'_z}{B_0} = 0.03 ;$$

or a consequence of formula (1):

$$\frac{B'_H}{B_0} = 0.165 .$$

This quantity is required to enable us to derive from the observations of the yellow radiation the altitude of the luminescent layer. Let h be this altitude. The brightness of the layer at the zenith distance z is the product of the brightness of the layer at the zenith and

[11] This calculation has been carried out previously by J. Dufay, thèse, p. 133, Paris, 1928.

of sec a, with $\sin a = (R/R + h) \sin z$ (R = the radius of the earth). We have, then, in the case of the luminescent layer,

$$\frac{B_H}{B_z} = \frac{T_H \sec a + \frac{B'_H}{B_0}}{T_z + \frac{B'_z}{B_0}} = 2.8 .$$

From this we conclude that sec $a = 3.83$.

The altitude of the luminescent layer would then be about 130 km.

VI. FREQUENCY OF THE TRANSITIONS $^2P \rightarrow {}^2S$ PER SECOND

The relation between the intensity of the yellow doublet and that of the green line of the aurora changes continually from one night to another and even during the same night. During the winter of 1935–1936 it varied from 0.85 to 1.3. But if we take as unity the average intensity of the green line, the average intensity of the yellow doublet has the value 0.48. Taking the value 1.35 erg/sec/m^2 for the average energy radiation of the green line in the south of France at the beginning of the winter of 1935–1936, we get for the yellow radiation 0.65 erg/sec/m^2, this being the energy released by 2.10^{11} transitions of the type $^2P \rightarrow {}^2S$.

VII. ON THE ORIGIN OF ATMOSPHERIC SODIUM

At 130 km above the earth the temperature of the atmosphere does not increase beyond 200° C. We cannot believe that a thermal effect explains the emission of the D lines. The problem is, moreover, twofold: What is the origin of the atmospheric sodium, and why does it become luminous in the upper atmosphere? We can examine whether the sodium atoms have a terrestrial or a cosmic origin. The first alternative seems to be untenable: we do not understand how a fine dust of sodium salt can be dissociated in its ascent from the ground to 130 km.

We tend to support the hypothesis of a cosmic origin. The earth receives each year from meteorites a deposit of 4 grams to the square kilometer. The proportion of sodium in weight is 7.2×10^{-3}. We receive then, per second and per square meter, 2.5×10^7 atoms of

sodium. It may be supposed that the yellow radiation of the night sky is a luminescent phenomenon accompanying the fall of the meteorites; in this case each sodium atom would undergo eight thousand transitions before definitely dying out.

The presence of sodium in the higher atmosphere, whatever may be its origin, leads us to look for other elements. In the stony meteorites, as in terrestrial rock, the most numerous atoms are[12] (after oxygen atoms) *Si*, *Mg*, *Fe*, *S*, *Al*, *Ca*, and *Ni*. We cannot expect anything from *Si*, *Mg*, and *S* atoms; the *Fe* lines are too numerous and consequently too weak. Only calcium and aluminum must give lines with marked intensity. The resonance line of the neutral *Ca* atom has the wave length 4226.73 A; we have actually observed a line of λ 4226 in the spectrum of the night sky. It would be interesting to investigate whether the bright emission lines of aluminum do not coincide with certain lines of the night-sky spectrum.

UNIVERSITÉ DE PARIS AND OBSERVATOIRE DE LYON
May 1938

[12] I. and W. Noddack, quoted by V. M. Goldschmidt, *Fortsch. d. Mineralogie*, **19**, 153, 1935.

ON THE INTENSITY DISTRIBUTION IN THE BANDS OF COMETARY SPECTRA

P. SWINGS AND M. NICOLET

ABSTRACT

The exceptional intensity distribution of bands of unsymmetrical molecules like *CN* and *CH* in a comet spectra can be explained by taking into consideration the following factors: (*a*) the frequency of electronic absorption processes; (*b*) the distribution in the vibrational levels (ground state) which is a function of the nuclear temperature T_1 or of the equivalent radiation temperature T_λ; (*c*) the distribution in the rotational levels corresponding to the nuclear temperature. These factors are different functions of the heliocentric distance r.

1. Important progress has been made in recent years in our knowledge of the physical mechanisms which take place in the atmospheres of the comets; the most outstanding contributions in this field are those of K. Wurm.[1] It seems useful to undertake a systematic rediscussion of the identifications of the emission bands observed in the spectra of comets; such a systematic work has been started in the department of astrophysics at Liége, Belgium.[2]

Actually, very great care must be taken in such identification work, as the intensity distributions and the structures of cometary bands differ widely from what we observe in normal laboratory spectra. This point has been advocated by Wurm on several occasions. In the course of our systematic discussions we had the feeling that there were still several points to be cleared up in connection with the prediction or discussion of the intensity distributions, as well as with the physical mechanisms present. The aim of this paper is to bring some precision into certain of these points. We shall restrict our considerations to the intensity distributions in rotational lines and vibrational bands of molecules which possess an electric dipole in their lowest electronic and vibrational state (such as *CN* or *CH*, but not C_2); the fundamental difference between the behaviors of the two types of molecules has been discussed by Wurm.

[1] Cf. *Zs. f. Ap.*, **15**, 115, 1938; *Handbuch d. Ap.*, **7**, 305, 1936.

[2] The first contribution of our department in this field has appeared recently; see M. Nicolet, "Les Bandes de *CH* et la présence de l'hydrogène dans les comètes," *Zs. f. Ap.*, **15**, 154, 1938. Other papers by Nicolet are in preparation.

Owing to the very low pressures prevailing in cometary atmospheres, the mean free path of the molecules is considerable. On the other hand, the excitation of the molecules has its primary origin in the solar radiation, the excitation by collisions being excluded. Under these conditions, what is the mechanism which prevails in the distribution of the molecules in the rotational levels of the lowest electronic and vibrational state?

2. Let r be the distance, in astronomical units, from the comet to the sun. By the application of Stefan's law, and assuming $T_\odot = 5740°$ K, it is found immediately[3] that a body absorbing the solar radiation at a distance r would take on a temperature[4] $T_1 \sim 300 r^{-1/2}$. But this factor, T_1, has no immediate meaning for the population in the discrete molecular levels in a gaseous atmosphere where collisions are practically absent.

3. We may, furthermore, try to find for different wave-length regions some kind of equivalent temperature T_λ in complete similarity with the case of interstellar matter;[5] this equivalent temperature T_λ must be such that the actual energy-intensity for wave-length λ is equal to that of equilibrium radiation at temperature T_λ. This treatment seems at first logical in this problem, owing to the selective absorption between the different rotational levels. Assuming that the sun radiates like a black body, and using the appropriate dilution factor, we find for the distribution in the excited levels, at the distance $r = 1$: for selective absorption at $\lambda \sim 4500$ A, the equivalent temperature $T_\lambda \sim 2000°$ K; for selective absorption at $\lambda \sim 1\mu$, the equivalent temperature $T_\lambda \sim 800°$; for selective absorption at $\lambda \sim 10\,\mu$, the equivalent temperature $T_\lambda \sim 70°$; for selective absorption at $\lambda \sim 100\,\mu$, the equivalent temperature $T_\lambda \sim 5°$. In any case, since the pure rotational lines of the molecules with which we are concerned lie in the region from 100 to 1000 μ or more, we should find by application of Boltzmann's law

[3] See, for instance, A. Adel, V. M. Slipher, and R. Ladenburg, *Ap. J.*, **86**, 345, 1937.

[4] For $T_\odot = 6000°$, T_1 would be $316 r^{-1/2}$, which means a difference of 16° at $r = 1$.

[5] A. S. Edington, *Internal Constitution of the Stars*, 2d ed., p. 371; for an application to the rotational levels of possible interstellar molecules, see P. Swings, *M.N.*, **97**, 212, 1937.

that all the molecules are practically in their lowest rotational level. This does not correspond with the observations.

4. Obviously, such a concentration in the lowest rotational level would be maintained only in the absence of perturbing processes. Collisions do not play any real role. But Wurm has called attention to an effect due to the electronic absorptions and emissions influencing the distributions in the rotational levels. He has shown that, owing to the differences in intensity of the R and P transitions in emission and absorption, higher rotational quantum numbers may be reached, as long as the frequency of the absorption processes in the photographic region is higher than $1/\tau_r$, τ_r being the lifetime of the rotational levels.

This mechanism presumably takes place, but it is not easy to predict its actual effect. On the other hand, the CN and CH molecules show a very different distribution; the CN molecules have their maximum population in the rotational levels near $K'' = 8$ (at $r = 1$), whereas the CH molecules are concentrated in the two or three lowest levels.[6] With Wurm's mechanism, the observed difference brings complications and probably implies quite different τ_r for CN and CH. We shall see later that, on the contrary, this difference appears conclusively when we assume another type of distributing mechanism.

5. It is possible to reach a result quite similar to that of Wurm by an alternative theory which enables an easy calculation of the effect in the general case; in fact, there are several other reasons which support our hypothesis and which will be developed in the following paragraphs.

The absorption of the solar radiation brings the cometary meteoric nucleus to a temperature T_1 given by the application of Stefan's law, following section 2. In the absence of any perturbing process the rotational populations of the lowest electronic level of any molecule will be practically the equilibrium distribution[7] cor-

[6] Following the identification by Nicolet, *loc. cit.*

[7] As a first approximation we may neglect here the dilution factor; thus, the equivalent temperature due to the nucleus is the same for all wave lengths. On the other hand, it is obvious that the frequency of transitions between rotational levels in equilibrium at approximately 300° is much higher than at $T_\lambda \sim 5°$ or less.

responding to $T_1 = 300r^{-1/2}$. The influence of the distance r is thus apparent.

In certain cases Wurm's mechanism may complicate somewhat the distribution in the lowest levels; but we may state that a rotational distribution corresponding to $T_1 = 300r^{-1/2}$ seems sufficient for the interpretation of the observed features, as will be seen later.[8]

6. We shall immediately show how simply our assumption explains the different distributions of the CN and CH molecules. These molecules have very different moments of inertia:

$$I''(CN) = 14.10^{-40} \text{ gm cm}^2 ;$$
$$I''(CH) = 2.10^{-40} \text{ gm cm}^2 .$$

Introducing these figures into the expression of the rotational energy in the Boltzmann factor, we find that they explain immediately the difference in distribution.

7. The problem may be different in the case of the vibrational levels. Let us assume a frequency of vibration $\omega'' = 1000 \text{ cm}^{-1}$. The first vibration-rotational bands will lie between $10\,\mu$ and $1\,\mu$; in this interval the equivalent temperature T_λ, following section 3, ranges from 70° to 800°. Thus, for the lowest levels the "nuclear" temperature T_1 will have the predominant effect, but not for the higher-lying vibrational states.

8. Summarizing the preceding considerations, we may say that, excluding intermittent or exceptional phenomena, the intensity of a cometary band depends upon the following factors: (*a*) the frequency of electronic absorption processes, which depends upon the spectral region and the structure of the absorption bands; (*b*) the distribution on the vibrational levels of the electronic ground state, which is a function either of the nuclear temperature T_1 (for the low quantum numbers v'') or of the equivalent temperatures T_λ (for high v''); (*c*) the distribution on the rotational levels corresponding to the nuclear temperature $T_1 = 300r^{-1/2}$. These factors are different functions of the distance r.

9. A verification of our hypothesis may be found in the good agreement obtained when we apply it to the identifications of CN

[8] An elementary calculation shows that the frequency of pure rotational transitions of molecules in equilibrium at $T_1 = 300°$ is at least as high as the frequency of electronic absorptions near λ 4500 for an equilibrium at $T_\lambda \sim 2000°$.

or *CH* lines or groups of lines.[9] We shall not give here all the details; these will be published by one of us (M. Nicolet).

For any identification the resolving-power of the spectrograph used[10] has to be considered first; the theoretical intensity of the rotational line must be examined next. Let Δ be the width in angstrom units of the monochromatic image of the slit on the plate. A convenient method for a first approach will be to represent each rotational line by a rectangle of width Δ and of height I, I being the theoretical intensity of the line. I is obtained immediately by classical formulae introducing the so-called intensity factor i and the Boltzmann expression. If Δ is smaller than the wave-length separation between two lines, these will appear separated on the spectrogram; but in the opposite case, the intensities will be distorted and may be represented by the sum of the rectangles which are superposed. Thus, we may find a blackening on the spectrogram, either (*a*) where the lines are very close together and not too weak (in the neighborhood of certain band heads) or (*b*) for the rotational quantum numbers giving maximum values of I. It may thus happen that a single branch will exhibit two marks on the plate: one near the head and one for the lines corresponding to the maximum values of I. For instance, the P branch of the (0, 0) transition of CN, which has a head, may show two maxima; inversely the R branch, which has no head, will exhibit only one maximum. In fact, this R branch is blended with the P branch of the (1, 1) transition; thus, when the emissions starting from $v' = 1$ are strong enough, this blending effect will complicate the aspect of the $R(0, 0)$ branch, although it is possible to interpret all the observed features.[11]

10. The main results concerning CN may be summarized as follows:

Let us take $\Delta = 2\,A$, which is approximately the case for the spectrograms of the Comet Brooks taken by W. H. Wright.[12] As-

[9] We may safely say that many identifications, even of molecules like *CN*, are incomplete or erroneous!

[10] We shall be concerned here exclusively with slit spectrograms.

[11] We want to emphasize the fact that the appearance of the spectrograms of the same comet obtained at the same moment with instruments of different resolving-power may be very different. See W. H. Wright, *Lick Obs. Bull.*, **7**, 8, 1912 (Comet Brooks).

[12] *Ibid.*, n. 11. Pl. No. 337: $\Delta = 1.9$ A; Pl. No. 338: $\Delta = 2.4$ A.

suming for T_1, respectively, 280° ($r \sim 1, 2$) and 420° ($r \sim 0, 5$), we have drawn diagrams of the intensity distributions in the (0, 0) bands in two cases: case A: without considering the effect of the (1, 1) transition; case B: with consideration of the effect of the $P(1, 1)$ branch on R (0, 0). These diagrams are shown in Figures 1, 2, and 3. The following results appear at once:

a) The band head[13] near λ 3881 has a rather sharp edge on the long wave-length side. Wurm has tentatively explained this phe-

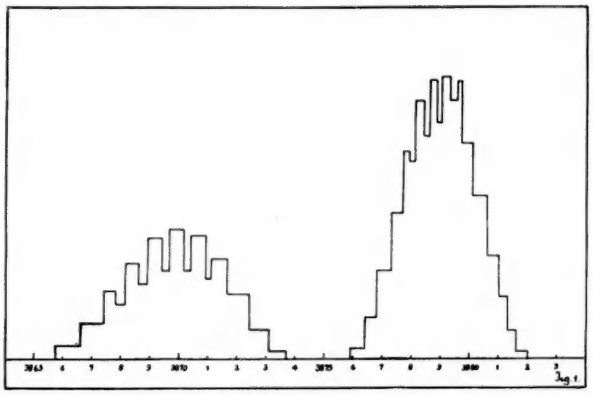

FIG. 1.—P and R branches of the (0, 0) transition in CN. $T_1 = 280°$ K. Without consideration of the $P(1, 1)$ band.

nomenon[14] by considering the intensity of the solar radiation and the density of the solar absorption lines in the exciting wave-length region. The effect mentioned here gives an alternative explanation; it is particularly conspicuous at $T_1 = 420°$ (see Fig. 2).

b) Beside the head at λ 3881, there is another maximum near λλ 3878–3879.[15] The head will be prominent at small distances r ($T_1 \sim 420°$); the opposite will happen at large distances ($T_1 \ll 300°$).

c) The band near λ 3870 is due to R(0, 0) in case A and to the blending of R(0, 0) and P(1, 1) in case B (Fig. 3). Case A corre-

[13] The laboratory head is at λ 3883.5.

[14] *Zs. f. Ap.*, **5**, 10, 1932.

[15] If $\Delta < 2$, this maximum may be separated from the band head; if $\Delta > 2$, the separation will disappear and the microphotometer structure will be different, the principal feature being either the head or the maximum.

sponds to great values of the distance r (low population of the vibrational level $v'' = 1$); Figure 1 gives us, then, a diffuse band with maximum at λλ 3869–3870. Case B will happen for small distances r; the maximum of case A at λ 3870 will then be distorted by another maximum of the P (1, 1) branch at λ 3868.

d) Thus, at a very small distance r we shall find simultaneously intensity maxima at λ 3881 (head of P[0, 0]) and λ 3868 (maximum of

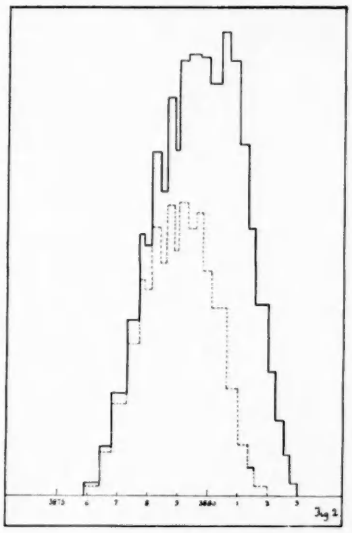

FIG. 2

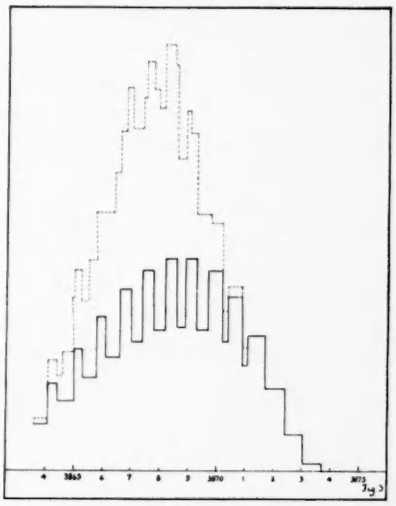

FIG. 3

FIG. 2.—P branch of the (0, 0) transition in CN. Continuous curve: $T_1 = 420°$ ($r \sim 0.5$); dotted curve: $T_1 = 280°$ ($r \sim 1.2$).

FIG. 3.—R branch of the (0, 0) transition in CN. Continuous curve: $T_1 = 420°$ without blending effect of P(1, 1); dotted curve: with consideration of P(1, 1), assuming for convenience I(1, 1) = ½I(0, 0) (I = intensity).

P[1, 1]); at a very large distance, intensity maxima will appear at λ 3879 (maximum of P[0, 0]) and λλ 3869–3870 (maximum of R[0, 0]).

e) Similar results are obtained for the bands near λ 4200, for which our assumption brings clearly an intensity-distribution quite identical to the (0, 0) band. The band head near λ 4215 is especially conspicuous for $T \geqslant 420°$, and the duplicity of the band at λ 4196 is due to the superposition of R(0, 1) and P(1, 2).

f) An examination of the wave lengths obtained with slit spectrograms[16] discloses a satisfactory agreement with the preceding considerations; of course, we have to consider carefully the effects of the distance r. Similarly, there is no difficulty in explaining certain differences between the spectra of different comets.

g) The subdivision of certain *CN* bands does not require special excitation processes of violent character; it is just a consequence of the preceding considerations.

h) Similarly, there is no need for two types of excitation, as suggested by A. Adel.[17] For Comet Zlatinsky ($r \sim 0.7$ a.u.) the band at λ 3881.1 corresponds, as has been stated by A. Adel and Wurm, to the wave lengths of the rotational lines P (13) or P (14) of the (0, 0) transition; but it is important to notice that actually the theoretically strongest line is P (8) or P (9); the observed effect is the result of the superposition of lines, owing to the value of Δ. This appears conclusively in the diagrams, as well as in the behavior with varying distance r.

i) It is obvious that a Boltzmann distribution at temperature T_1 is only a first, and possibly rather crude, approximation. The population in the lowest rotational level may be higher than in the case of a true Boltzmann distribution. If so, the lines observed near λλ 3864, 3873, and 4190 could be, respectively, the origins of the (0, 0), (1, 1), and (1, 2) transitions.

j) A careful investigation of the red system of *CN* in comets is still lacking, the actual data by F. Baldet,[18] N. T. Bobrovnikoff,[19] Dufay, Bloch, and Ellsworth,[20] J. Gauzit,[21] and R. Minkowski[22] be-

[16] Comet Daniel: Campbell, *Ap. J.*, **28**, 229, 1908; Comet Brooks: Wright, *Lick Obs. Bull.*, *loc. cit.*; Comet Beliavsky: Bobrovnikoff, *Pub. A.S.P.*, **43**, 61, 1931; Comet Zlatinsky: Slipher, *Lowell Obs. Bull.*, **2**, 67, 1914; Comet Delavan: Curtiss and McLaughlin, *Pub. U. Michigan*, **3**, 263, 1923; Comet Mellish: Slipher, *op. cit.*, p. 151, 1916; Comet Finsler: Minkowski, *Pub. A.S.P.*, **49**, 276, 1937; Comet Halley: Bobrovnikoff, *Pub. Lick Obs.*, **17**, 443, 1931.

[17] A. Adel, *Pub. A.S.P.*, **49**, 254, 1937.

[18] F. Baldet, thèse, Paris (*Annales de Meudon*, **7**, I, 1926).

[19] Bobrovnikoff, *op. cit.*, n. 16.

[20] Dufay, Bloch, et Ellsworth, *C.R.*, **204**, 663, 1937; *J. de Phys.*, **8**, 17, 1937.

[21] J. Gauzit, *C.R.*, **206**, 169, 1938.

[22] Minkowski, *op. cit.*, n. 16.

ing only preliminary in character. Owing to the different electronic transition ($^2\Pi \rightarrow {}^2\Sigma$ instead of $^2\Sigma \rightarrow {}^2\Sigma$), the intensity distributions among vibrational bands, as well as the rotational lines, must be quite different.

11. The identification of *CH* by M. Nicolet[23] was based on the same principle. Adopting $\Delta = 2A$ and $T_1 = 300°$, we obtain Figure 4.

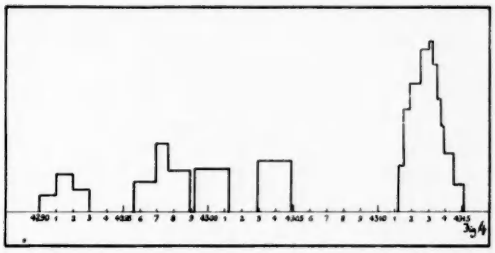

FIG. 4.—Intensity distribution in *CH* between λ 4290 and λ 4315 A. $T_1 = 300°$

This explains at once the following features: (*a*) λ 4313 is a rather narrow and strong emission; (*b*) λ 4297 and λ 4291.5 are blends of two rotational lines; the intensity of λ 4297 is similar to that of the single line λ 4304; (*c*) when $\Delta > 2A$, a single band is observed from λ 4296 to λ 4301 (blend of three lines).

A discussion of the other electronic transition $B\ ^2\Sigma \rightarrow X\ ^2\Pi$ of *CH* will be published later by one of us (M. Nicolet).

UNIVERSITY OF LIÉGE
DEPARTMENT OF ASTROPHYSICS
April 1938

[23] Nicolet, *loc. cit.*

THE ANALYSIS OF THE INFRARED LIMIT OF ATMOSPHERIC TRANSMISSION

ARTHUR ADEL AND C. O. LAMPLAND

ABSTRACT

The correspondence between the related set of carbon dioxide bands at 15 μ and the infrared limit of atmospheric transmission is discussed in detail. A sample curve of atmospheric transmission in this spectral region is given by way of illustration of the detail actually present in what had formerly been considered a featureless, smooth curve.

Description of the rock-salt prismatic solar spectrum in the neighborhood of the infrared cutoff.—The appearance of the long wavelength end of the telluric spectrum may be briefly reviewed as follows. It is characterized principally by the powerful absorption of ozone at 9.6 μ, the cutoff in the vicinity of 14 μ, and the two small absorption bands q_1 and q_2 between.[1] It is the purpose of this paper to specify more precisely the character of the infrared limit of atmospheric transmission.

The infrared limit of transmission.—Figure 1 is a reproduction from the work of Martin and Barker of the related set of carbon dioxide absorption bands at 15 μ.[2] The atmospheric opacity in question is produced by carbon dioxide by virtue of the existence of this set of bands.[3] A high resolving-power curve of a portion of this region, also from the work of Martin and Barker, is shown as Part *a* of Figure 2. Part *b* of Figure 2 is the corresponding section of the rock-salt prismatic solar spectrum . Part *b* was recorded at the Lowell Observatory on May 9, 1938, during the interval 10:35–11:00 A.M., M.S.T. The sky was clear. The connecting lines in the figure indicate the corresponding regions of absorption.

General remarks concerning the absorption bands.—The identification of the bands is well known and is given in connection with Figure 1.

[1] A. Adel and C. O. Lampland, *Ap. J.*, **87**, 198, 1938.

[2] *Phys. Rev.*, **41**, 291, 1932.

[3] A rather weak absorption band of ozone with its center at 14.2 μ contributes slightly to the cutoff.

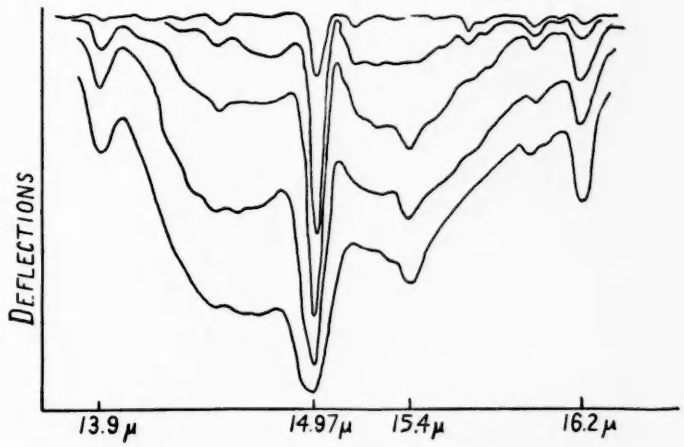

FIG. 1.—The absorption of infrared radiation by carbon dioxide at 15 μ

IDENTIFICATION OF THE SET OF CARBON DIOXIDE BANDS AT 15 μ

λ (μ)	Transition $(V_1\ V_2\ l) \rightarrow (V_1'\ V_2'\ l')$
14.97	0 0 0 → 0 1 1
	0 1 1 → 0 2 2
	0 2 2 → 0 3 3
16.17, 13.89	0 1 1 → {0 2 0; 1 0 0}
16.74, 13.48	0 2 2 → {0 3 1; 1 1 1}
18.34, 15.46, 14.50, 12.64	{□ 2 0; 1 0 □} → {0 3 1; 1 2 1}

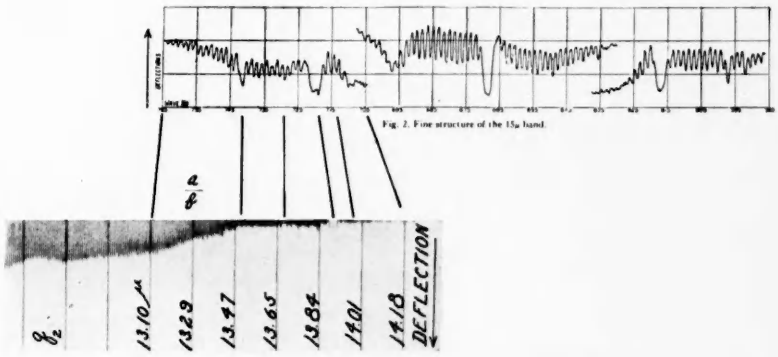

FIG. 2.—The infrared limit of atmospheric transmission

It can be shown that the matrix element of the electric moment for each of these transitions is of the order of β, where $\beta e^{i\varphi}$ is the component of the electric moment perpendicular to the symmetry axis

TABLE 1

Wave-Length Interval	Approximate Percentage Transmission
13.10–13.29	85
13.29–13.47	60
13.47–13.65	27
13.65–13.84	33
13.84–14.00	15
14.00–14.12	8
13.10–14.12	41

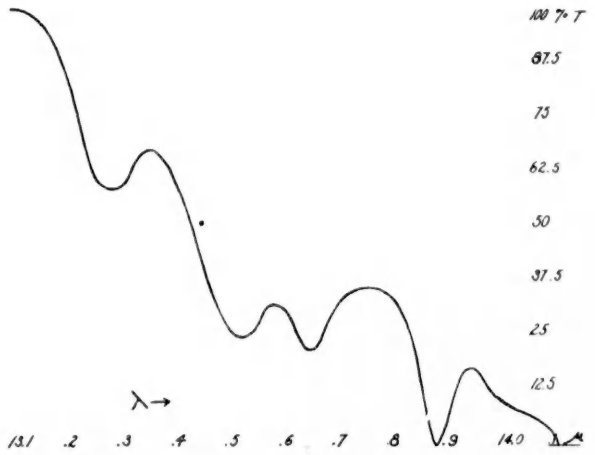

FIG. 3.—Atmospheric transmission at the cutoff

of the molecule. The intensities of the absorption bands will therefore be in the same relation as the molecular populations of the several initial levels. This fact explains the near-symmetrical nature of the laboratory-curves shown in Figures 1 and 2.

Concluding remarks.—The apparent percentage transmission of our atmosphere in this region of the spectrum can be obtained by extending the indicated envelope of the sun's energy-curve. The results are summarized approximately in Table 1 and in Figure 3 for the atmospheric curve shown in Part *b* of Figure 2. This curve of transmission will vary, of course, with the zenith distance of the sun. It may perhaps vary with the season and with the location of the observing station.

LOWELL OBSERVATORY
FLAGSTAFF, ARIZONA
June 1938

FURTHER DETAIL IN THE ROCK-SALT PRISMATIC SOLAR SPECTRUM

ARTHUR ADEL

ABSTRACT

New features in the infrared telluric spectrum, made apparent with increased resolving-power, are briefly discussed.

Envelope structure of the ozone band at 9.6 μ.—With increased resolving-power it has been possible to disclose further detail in the rock-salt prismatic solar spectrum.[1]

We note in Part *a* of Figure 1, for example, that the envelope structure of the strong ozone band at 9.6 μ is clearly that of a doublet. The character of the envelope of this absorption band is of considerable importance in deducing the structure of the ozone molecule and in analyzing the latter's infrared spectrum.[2] The present prismatic measures, made at the Lowell Observatory, corroborate the grating measures made at the University of Michigan in 1935, in which this envelope form was first revealed.[2] The grating observations, which placed the band center at 9.57 μ, are shown in Part *b* of Figure 1.

Detail in the spectral interval from 7.2 to 8.5 μ.—Of greater importance is the disclosure of additional absorption bands in the vicinity of the diverging wall of the great water band ν_2. The new curve is shown in Figure 2. Definite identifications are postponed for the future. As a preliminary, however, it may be instructive to point out the possibility that these new bands may indicate the existence of additional oxides of nitrogen in the atmosphere. For example, the molecule of N_2O possesses two doublet bands with centers at 7.77 and 8.57 μ, the former being more than twice as intense as the latter.[3] It may well be that the *R* branch of the N_2O

[1] For a description of the telluric spectrum please see *Ap. J.*, **87**, 198, 1938.

[2] A. Adel, V. M. Slipher, and O. Fouts, *Phys. Rev.*, **49**, 288, 1936.

[3] E. K. Plyler and E. F. Barker, *Phys. Rev.*, **38**, 1827, 1931.

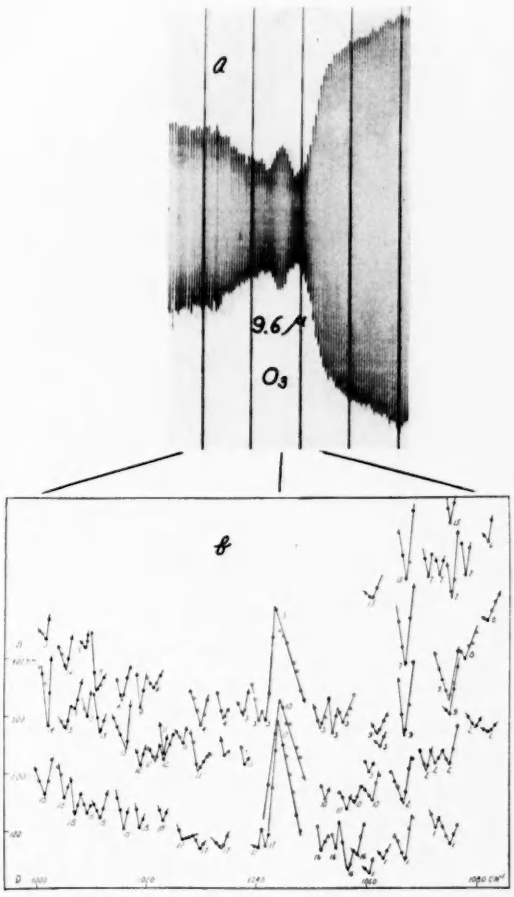

FIG. 1.—Envelope structure of the ozone band at 9.6 μ

band at 7.77 μ and the N_2O_5 band at 7.6 μ combine to form the telluric absorption with its center at 7.63 μ.[1]

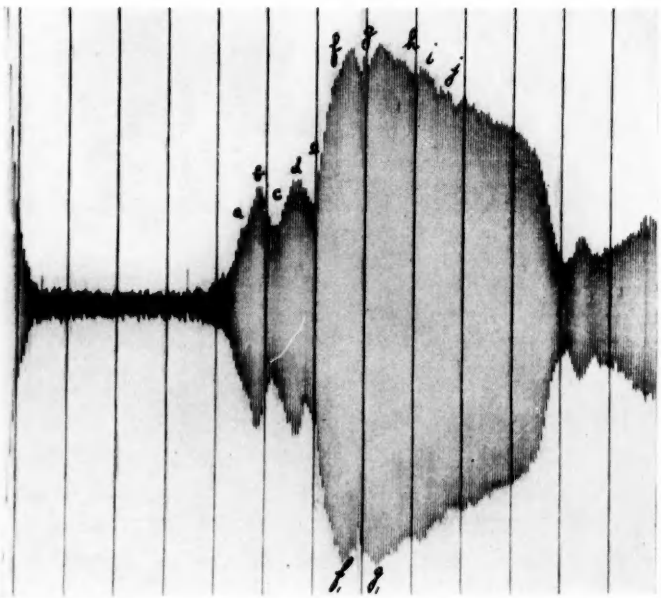

FIG. 2.—Detail in the spectral interval from 7.2 to 8.5 μ

Detail	λ (μ)	Detail	λ (μ)
a	7.44	f_1	8.10
b	7.55	*g*	8.17
c	7.63	g_1	8.30
d	7.77	*h*	8.48
e	7.85	*i*	8.58
f	8.05	*j*	8.72

The wave-lengths are approximate. It should be remarked also that the deflections at the base of the great water band are probably spurious. The detail enumerated in this table and shown in Fig. 2 has been observed regularly since its discovery.

LOWELL OBSERVATORY
FLAGSTAFF, ARIZONA
June 1938

NONRADIAL OSCILLATIONS OF STARS

PART I

C. L. PEKERIS

ABSTRACT

In the first part of this paper a derivation is given of the Eulerian equations which govern the small and adiabatic oscillations of a general spherical harmonic type of nonrotating stars. These equations are then solved for a model of constant density. It is shown that with the exception of purely radial oscillations, which are unstable only when $\gamma < \frac{4}{3}$, there exist nonradial modes of oscillation, which are unstable for all values of γ. The conclusion is drawn that in the pulsation theory of stellar variability it is necessary to consider nonradial disturbances in order to ascertain the possibility of the existence of any assumed model.

1. INTRODUCTION

In current theoretical discussions of stellar pulsation it is customary to leave out of consideration nonradial modes of oscillation, with the justification that these modes are likely to be associated with a greater amount of viscous damping than purely radial oscillations. It may be argued, however, that in the lowest modes of nonradial oscillation the viscous damping is not likely to exceed by a great deal the damping in radial oscillations. Furthermore, we must consider the circumstance that, whatever external disturbances may exist, they will always be of a nonradial character. More serious, however, is the fact, pointed out by Rosseland,[1] that a limitation to purely radial oscillations fails to reveal the possible instability of the assumed model for a more general type of disturbance. If there is any mode of oscillation for which the assumed model is unstable, then the possibility of the existence of a star built on that model is nil; and therefore the periods of purely radial oscillations of the model can have no application to actual stars. An investigation of nonradial oscillations should thus lead to an elimination of a large class of stellar models and would further add significance to the computed periods of radial oscillation of those models which prove to be stable. Among other problems which can only be solved by considering nonradial oscillations is, for example, the question of the degree of

[1] S. Rosseland, *Oslo Obs. Pub.*, **1**, No. 2, 2, 1932.

instability of a star consisting of an adiabatically unstable core and a stable shell.

In the following we derive the Eulerian equations which govern the small adiabatic oscillations of nonrotating stars. This problem was treated by Rosseland[2] in connection with his investigation of the effect of nonadiabatic processes on the stability of stars, but he made a special assumption concerning the functional form of the variable part of gravity. The variation with latitude and longitude of any mode of oscillation is given by a factor of a surface spherical harmonic, and we shall henceforth distinguish between the various modes by the order of this spherical harmonic. It is shown that the oscillations are governed by an ordinary differential equation of the fourth order. In the special case of a model of constant density this equation reduces to a system of two simultaneous equations of the second order, the solution of which is given. This solution yields, first, the known frequencies of purely radial oscillations, which are stable provided $\gamma > \frac{4}{3}$. The nonradial oscillations are, for any given spherical harmonic, either of a stable or an unstable type. The existence of these nonradial stable modes for a model of constant density is at first surprising, but an examination of one pair of modes for the spherical harmonic of the second order shows that in the stable case the destabilizing forces act in opposite directions in the central and outer parts of the star, thus neutralizing each other. In the unstable mode the motion is such that the destabilizing forces in the two parts of the star reinforce each other. It must be emphasized, however, that the existence of stable modes of oscillation is of no consequence if there also are other modes which are unstable, because under any type of disturbance, except of one class of extremely special nature, the unstable modes will grow exponentially with time relative to the stable modes and will eventually cause a transition from the originally assumed configuration to another one.

2. THE THEORY OF SMALL ADIABATIC OSCILLATIONS OF FLUID GLOBES

The limitation to small oscillations implies that the amplitudes of the velocities and of their derivatives are assumed to be so small that

[2] *Ibid.*, p. 12.

their squares and products can be neglected in comparison with their first powers. We also neglect viscous forces and assume that the motion of any individual particle occurs adiabatically. In spherical co-ordinates let w, u, and v designate respectively the radial, latitudinal, and longitudinal components of velocity. Further, let the subscript "o" refer to the equilibrium value of any quantity, and let a symbol without a subscript stand for the perturbed part of that quantity. Then with

$$\mathrm{X} = \frac{1}{r^2}\frac{\partial}{\partial r}(r^2 w) + \frac{1}{r \sin\theta}\frac{\partial}{\partial \theta}(\sin\theta u) + \frac{1}{r \sin\theta}\frac{\partial v}{\partial \varphi}, \tag{1}$$

the equation of continuity,

$$\frac{D(\rho_0 + \rho)}{Dt} = -(\rho_0 + \rho)\mathrm{X}, \tag{2}$$

reduces under the foregoing assumptions to

$$\frac{\partial \rho}{\partial t} = -w\frac{\partial \rho_0}{\partial r} - \rho_0 \mathrm{X}. \tag{3}$$

For an ordinary gas the condition of adiabatic motion is expressed by

$$\frac{1}{(p_0 + p)}\frac{D(p_0 + p)}{Dt} = \frac{\gamma}{(\rho_0 + \rho)}\frac{D(\rho_0 + \rho)}{Dt}, \tag{4}$$

where γ is the ratio of specific heat at constant pressure and constant volume. Under stellar conditions γ is a variable quantity, but the limits of its possible variation are relatively small and we shall assume for simplicity that it is constant. It will also be convenient to introduce the quantity c, having the dimension of a velocity, defined by

$$c^2 = \gamma \frac{p_0}{\rho_0}. \tag{5}$$

In an ordinary gas, c is the Laplacian velocity of sound. Thus, (4) becomes

$$\frac{\partial p}{\partial t} + w\frac{\partial p_0}{\partial r} = c^2\left(\frac{\partial \rho}{\partial t} + w\frac{\partial \rho_0}{\partial r}\right) = -\rho_0 c^2 \mathrm{X} . \tag{6}$$

Remembering that

$$\frac{\partial p_0}{\partial r} = -g_0\rho_0 ,$$

we obtain from (6)

$$\frac{\partial p}{\partial t} = \rho_0(g_0 w - c^2\mathrm{X}) . \tag{7}$$

The gravitational potential will consist of an equilibrium part, ψ_0, and a perturbed part, ψ, which satisfy, respectively, the equations

$$\left.\begin{aligned} \nabla^2\psi_0 &= -4\pi G\rho_0 , \\ \nabla^2\psi &= -4\pi G\rho . \end{aligned}\right\} \tag{8}$$

Again, on neglecting quantities of the second order, the equations of motion become

$$\rho_0\frac{\partial u}{\partial t} = -\frac{1}{r}\frac{\partial}{\partial t}(p - \rho_0\psi) , \tag{9}$$

$$\rho_0\frac{\partial v}{\partial t} = -\frac{1}{r\sin\theta}\frac{\partial}{\partial \varphi}(p - \rho_0\psi) , \tag{10}$$

$$\rho_0\frac{\partial w}{\partial t} = -\frac{\partial p}{\partial r} + \rho_0\frac{\partial \psi}{\partial r} - g_0\rho . \tag{11}$$

We now assume that the dependence of each of the perturbed quantities upon time is given by a factor $e^{i\sigma t}$, where the real part of σ stands for $(2\pi/T)$, T being the period. Any possible mode of oscillation will be characterized by an appropriate value of σ, which will in general be complex; and the mode will be stable, unstable, or neutral if the imaginary part of σ is, respectivey, positive, negative, or

zero. By differentiating (11) with respect to t and (7) with respect to r, we obtain, with the aid of (3),

$$\sigma^2 w - \dot{g}_0 w - g_0 \dot{w} + i\sigma\dot{\psi} + c^2\dot{\mathrm{X}} + g_0(1-\gamma)\,\mathrm{X} = 0\,. \tag{12}$$

Now substitute for u and v in (1) from (9) and (10), obtaining

$$\mathrm{X} = \frac{1}{r^2}\frac{\partial}{\partial r}(r^2 w) + \frac{i}{\sigma r^2}\left\{\frac{1}{\sin\theta}\frac{\partial}{\partial\theta}\left(\sin\theta\,\frac{\partial}{\partial\theta}\right) + \frac{1}{\sin^2\theta}\frac{\partial^2}{\partial\varphi^2}\right\}\left(\frac{p}{\rho_0} - \psi\right). \tag{13}$$

If the dependence of the perturbed quantities on θ and φ be given by a spherical surface harmonic of order n, then the operator in $\{\ \}$ is equal to $-n(n+1)$. Thus, with the aid of (7), (13) becomes

$$\mathrm{X} = \frac{1}{r^2}\frac{\partial}{\partial r}(r^2 w) - \frac{n(n+1)}{\sigma^2 r^2}(g_0 w - c^2\mathrm{X}) + \frac{in(n+1)}{\sigma r^2}\psi\,,$$

or

$$\left.\begin{aligned} r^2\dot{w} + w\left[2r - g_0(n+1)\frac{n}{\sigma^2}\right] + in(n+1)\frac{\psi}{\sigma} \\ = \mathrm{X}\left[r^2 - n(n+1)\frac{c^2}{\sigma^2}\right]. \end{aligned}\right\} \tag{14}$$

Finally, on differentiating (8) with respect to t, we obtain

$$i\sigma\nabla^2\psi = -4\pi G\frac{\partial\rho}{\partial t} = 4\pi G\left(w\frac{\partial\rho_0}{\partial r} + \rho_0\mathrm{X}\right). \tag{15}$$

We now proceed to eliminate ψ from the system of equations (12), (14), and (15). First we compute $\nabla^2\psi$ from (12) and (14) and substitute in (15), obtaining

$$\left.\begin{aligned} c^2\ddot{\mathrm{X}} + \dot{\mathrm{X}}\left[c^2 - (\gamma-1)g + \frac{2c^2}{r}\right] \\ + \mathrm{X}\left\{\sigma^2 + (2-\gamma)\left(\dot{g} + \frac{2g}{r}\right) - n(n+1)\frac{c^2}{r^2}\right\} \\ = g\ddot{w} + \dot{w}\left(2\dot{g} + \frac{2g}{r}\right) + [2 - n(n+1)]\frac{wg}{r^2}\,. \end{aligned}\right\} \tag{16}$$

On differentiating (14), one obtains,[3] with the aid of (12),

$$\left.\begin{aligned}\dot{\mathrm{X}}r^2 + \mathrm{X}\left[2r + (g - \gamma g - c^2)(n+1)\frac{n}{\sigma^2}\right] \\ = r^2\ddot{w} + 4r\dot{w} + w[2 - n(n+1)]\,.\end{aligned}\right\} \quad (17)$$

The elimination of w from the last two equations is rather cumbersome, and we shall give only the final result. Let

$$A = 2\left(\frac{\dot{g}}{g} - \frac{1}{r}\right), \qquad gG = c^2\ddot{\mathrm{X}} + \dot{\mathrm{X}}\left(\dot{c}^2 - \gamma g + \frac{2c^2}{r}\right)$$
$$+ \mathrm{X}\left[\sigma^2 + (2-\gamma)\dot{g} + (1-\gamma)\frac{2}{r} - n(n+1)\frac{c^2}{gr^2}\right.$$
$$\left. + \frac{n}{\sigma^2 r^2}(n+1)(\dot{c}^2 - g + \gamma g)\right],$$
$$H = \ddot{\mathrm{X}} + \dot{\mathrm{X}}\left[\frac{4}{r} - \frac{n}{\sigma^2 r^2}(n+1)(\dot{c}^2 - g + \gamma g)\right]$$
$$+ \mathrm{X}\left[\frac{2}{r^2} - \frac{n}{\sigma^2 r^2}(n+1)(\ddot{c}^2 - \dot{g} + \gamma\dot{g})\right];$$

then

$$\left.\begin{aligned}\ddot{G} + \dot{G}\left(\frac{6}{r} - 2\frac{\dot{A}}{A}\right) + G\left\{-\frac{\ddot{A}}{A} + \left(\frac{6 - n - n^2}{r^2}\right) - \frac{6\dot{A}}{Ar} + \frac{2\dot{A}^2}{A^2}\right\} \\ - AH = 0\,.\end{aligned}\right\} \quad (18)$$

The boundary conditions are, in the case of a star of finite radius, first, that X shall be regular everywhere. At the boundary ($r = R$), $D(p_0 + p)/Dt$ must vanish. But by (6) this is equal to $-\rho_0 c^2 \mathrm{X}$ or to $-\gamma p_0 \mathrm{X}$; and, since p_0 vanishes there, the foregoing condition will be satisfied if X does not become infinite. We have an additional condition arising from the fitting of the perturbed gravitational potential at the boundary. Let the dependence on r of the gravitational potential inside and outside the star be denoted, respectively, by ψ and ψ'; then, corresponding to any spherical harmonic n, the latter will be

[3] From now on we shall omit the subscript in g_0.

of the form (C/r^{n+1}). The continuity of the gravitational potential at R requires that

$$\frac{C}{R^{n+1}} = \psi_R \,. \tag{19}$$

If, now, η denotes the amplitude of the deviation of the boundary from its equilibrium value R, we have the additional condition that

$$\left(\frac{\partial\psi}{\partial r} - \frac{\partial\psi'}{\partial r}\right)_R = 4\pi G(\rho_0\eta)_R \,,$$

or

$$i\sigma\left(\frac{\partial\psi}{\partial r} - \frac{\partial\psi'}{\partial r}\right)_R = 4\pi G(\rho_0 w)_R \,. \tag{20}$$

But

$$\left(\frac{\partial\psi'}{\partial r}\right)_R = -(n+1)\frac{C}{R^{n+2}} = -(n+1)\frac{\psi_R}{R} \,,$$

so that (20) becomes

$$i\sigma\left[\frac{\partial\psi}{\partial r} + (n+1)\frac{\psi}{R}\right]_R = 4\pi G(\rho_0 w)_R \,. \tag{21}$$

The foregoing system suffices to determine uniquely the state of motion of a star when perturbed slightly from its equilibrium configuration, as will be illustrated in one simple case in the next section. Before doing so, we shall verify that our equations agree with the Lagrangian equation of the second order, which is known to control purely radial oscillations. When $n = 0$, (14) reduces to

$$\mathrm{X} = \dot{w} + \frac{2w}{r} \tag{22}$$

and (15) integrates to

$$i\sigma\dot{\psi} = 4\pi G\rho_0 w \,, \tag{23}$$

which, when substituted in (12), yields the equation

$$D(w) \equiv c^2\ddot{w} + \dot{w}\left(\frac{2c^2}{r} - \gamma g\right) + w\left[\sigma^2 - \frac{2c^2}{r^2} + (2-\gamma)\frac{2g}{r}\right] = 0. \quad (24)$$

By making the substitution $w = rf(r)$ in (24), we obtain an equation for f:

$$c^2\ddot{f} + \dot{f}\left(\frac{4c^2}{r} - \gamma g\right) + f\left[\sigma^2 + (4-3\gamma)\frac{g}{r}\right] = 0, \quad (25)$$

which is identical with the one in Eddington's theory of radial oscillations. Equation (17) reduces to the result of multiplying (22) by r^2 and differentiating once, while equation (16) reduces to

$$\left(\frac{d}{dr} + \frac{2}{r}\right) Dw = 0.$$

3. NONRADIAL OSCILLATIONS OF A MODEL OF CONSTANT DENSITY

Let $A = (4\pi/3)G\rho_0$, $\beta = (\sigma^2/A)$; then

$$g_0 = Ar, \qquad p_0 = \tfrac{1}{2}A\rho_0(R^2 - r^2), \qquad c^2 = \frac{\gamma}{2}A(R^2 - r^2),$$

and the right-hand sides of (16) and (17) become, respectively,

$$Ar\left\{\ddot{w} + \frac{4}{r}\dot{w} + [2 - n(n+1)]\frac{w}{r^2}\right\},$$

$$r^2\left\{\ddot{w} + \frac{4}{r}\dot{w} + [2 - n(n+1)]\frac{w}{r^2}\right\}.$$

Thus, on eliminating the expression in { } between (16) and (17), we obtain

$$\left.\begin{aligned}(R^2 - r^2)\ddot{X} + \frac{\dot{X}}{r}(2R^2 - 6r^2) + X\left[\frac{2\beta}{\gamma} + \frac{8}{\gamma} - 6 - (n+1)\frac{2n}{\gamma\beta}\right.\\ \left. - (n+1)\frac{n}{r^2}(R^2 - r^2)\right] = 0.\end{aligned}\right\} \quad (26)$$

It will be convenient to introduce the nondimensional co-ordinate $y = (r/R)$, whereby (20) transforms into

$$\left.\begin{aligned}(1 - y^2)\ddot{\mathrm{X}} + \frac{\dot{\mathrm{X}}}{y}(2 - 6y^2) \\ + \mathrm{X}\left[\frac{2\beta}{\gamma} + \frac{8}{\gamma} - 6 - (n+1)\frac{2n}{\gamma\beta} - (n+1)\frac{n}{y^2}(1 - y^2)\right] = 0 .\end{aligned}\right\} \quad (27)$$

Having solved (27), ψ can be determined from (15), which reduces to

$$i\sigma\nabla^2\psi = 3A\mathrm{X} , \quad (28)$$

and then w can be determined by eliminating $\dot{w}$ between (12) and (14). Now, the solutions of X behave at the origin like r^n or r^{-n-1}. Hence, we write $\mathrm{X} = y^n F(y)$, and substitute it in (27), obtaining

$$(1 - y^2)\ddot{F} + \frac{\dot{F}}{y}[2n + 2 - y^2(2n + 6)] + BF = 0 , \quad (29)$$

where $B = -6 - 4n + (8/\gamma) + (2\beta/\gamma) - 2(n+1)(n/\gamma\beta)$. Let $F = \sum_0^\infty c_n y^n$; then it follows from (29) that

$$c_{k+2} = c_k \left\{ \frac{k(k + 5 + 2n) - B}{(k+2)(k+3+2n)} \right\} . \quad (30)$$

When k becomes large, (c_{k+2}/c_k) approaches unity, and it can be shown that F will not converge at $y = 1$. Hence, in order to make $\mathrm{X}(1)$ finite, we must have

$$B = k(k + 5 + 2n) , \qquad k = 0, 2, 4 \ldots , \quad (31)$$

and F will be a polynomial of degree k. Equation (31) may be written in the form

$$\beta - (n+1)\frac{n}{\beta} = -4 + \frac{\gamma}{2}[k(k + 5 + 2n) + 6 + 4n] \equiv 2D ,$$

or

$$\beta = D \pm [D^2 + n(n+1)]^{\frac{1}{2}} . \tag{32}$$

It is clear that, no matter what the values of k and γ may be, there is always one value of β which is negative, implying an unstable mode of oscillation. When $n = 0$, the relevant root is

$$\beta = 2D = 3\gamma - 4 + \frac{\gamma}{2} k(k+5) , \tag{33}$$

as can be ascertained directly from (27). Equation (33) shows that in the mode without nodes, for which $k = 0$, β becomes negative when $\gamma < \frac{4}{3}$, a result which was first derived by Ritter.

To obtain more insight into the nature of the modes which correspond respectively to the two possible values of β when $n \neq 0$, we shall study the case $n = 2$, $k = 0$. We have

$$2D = 7\gamma - 4 , \qquad X = Cr^2 ,$$

$$i\sigma\nabla^2\psi = i\sigma\left(\ddot{\psi} + \frac{2\dot{\psi}}{r} - \frac{6\psi}{r^2}\right) = 3AX = 3ACr^2 .$$

Hence,

$$i\sigma\psi = \tfrac{3}{14}ACr^4 + Er^2 , \tag{34}$$

where C and E are arbitrary constants. It follows from (12) and (14) that

$$\left.\begin{aligned} w\left[\sigma^2 r^2 - r^2\dot{g} + 2rg - n(n+1)\frac{g^2}{\sigma^2}\right] &= -c^2 r^2 \dot{X} \\ &+ X\left[\gamma r^2 g - n(n+1)c^2\frac{g}{\sigma^2}\right] - i\sigma r^2\dot{\psi} - in(n+1)\psi\frac{g}{\sigma} , \end{aligned}\right\} \tag{35}$$

where the dots stand for differentiation with respect to r. In our case, (35) reduces to

$$\left.\begin{aligned} \left[\beta + 1 - (n+1)\frac{n}{\beta}\right]w = (7\gamma - 3)w = -\frac{\gamma}{2}(R^2 - r^2)\dot{X} \\ + X\left[\gamma r - \gamma(n+1)(R^2 - r^2)\frac{n}{2\beta r}\right] - i\frac{\sigma}{A}\dot{\psi} - in(n+1)\frac{\psi}{r\sigma} . \end{aligned}\right\} \tag{36}$$

The constant E in (34) can now be evaluated by substituting the value of w_R from (36) in (21), the result being

$$E = -\tfrac{3}{14}ACR^2 .$$

Hence,

$$\psi = \tfrac{3}{14}ACr^2(r^2 - R^2) \tag{37}$$

and

$$w = CR^2 \frac{r}{7}\left\{\frac{r^2}{R^2}\left(2 + \frac{3}{\beta}\right) - 1 - \frac{3}{\beta}\right\} . \tag{38}$$

The expressions in $\{\ \}$ for $\gamma = (5/3)$ and $(4/3)$ are given in Table 1, where the superscripts $(^+)$ and $(^-)$ refer, respectively, to the positive

TABLE 1

γ	β^+	$\{\ \}^+$	β^-	$\{\ \}^-$
5/3	8.38	$2.36(r^2/R^2)-1.36$	−0.716	$-2.19(r^2/R^2)+3.19$
4/3	6.29	$2.48(r^2/R^2)-1.48$	−0.954	$-1.14(r^2/R^2)+2.14$

and negative roots of (32). It is seen that in the stable solutions (positive β) w changes sign in the interior of the star, while in the unstable solutions it does not. The stability of the former solutions is thus to be explained by the neutralization of the opposing destabilizing forces in the central and outer portions of the star. Similar results are found in the case $n = 1$, $k = 0$. These modes are distinguished from all the others by the fact that w does not vanish at the origin, which simply expresses the fact that a deformation of the form of a spherical harmonic of the first order is equivalent to a shifting of the center of mass.

Further applications of the foregoing theory to other models will be made in a forthcoming paper.

I wish to express my appreciation of the interest shown by Professor S. Chandrasekhar in this and in other problems of stellar hydrodynamics, and to thank Professor O. Struve for the opportunity to spend some time at the Yerkes Observatory.

YERKES OBSERVATORY AND MASSACHUSETTS
INSTITUTE OF TECHNOLOGY
June 15, 1938

NOTES

ORIGIN OF THE INFRARED TELLURIC ABSORPTION BAND q_2

ABSTRACT

It is demonstrated that the telluric absorption band at 12.65 μ is a member of the family of carbon dioxide bands which determine the infrared limit of atmospheric transmission.

Observations of the telluric spectrum made at the University of Michigan several years ago disclosed a moderately intense absorption band in the neighborhood of 12.5 μ.[1] Recent measures at the Lowell Observatory confirm the existence of the band and provide the position 12.65 μ for its center.[2]

The rather abrupt cessation of atmospheric transmission indicated by the Michigan observations at 13.5 μ has also been confirmed by the Lowell measures. A detailed analysis of this cutoff now in progress at this observatory has revealed the important role played by the upper-stage transitions:

$$(\nu_2)_1 \rightarrow \begin{pmatrix} 2\nu_2 \\ \nu_1 \end{pmatrix}_0 ; \qquad \begin{pmatrix} 2\nu_2 \\ \nu_1 \end{pmatrix}_0 \rightarrow \begin{pmatrix} 3\nu_2 \\ \nu_2 + \nu_1 \end{pmatrix}_1 ; \qquad \begin{pmatrix} 3\nu_2 \\ \nu_2 + \nu_1 \end{pmatrix}_1 \rightarrow \begin{pmatrix} 4\nu_2 \\ 2\nu_2 + \nu_1 \\ 2\nu_1 \end{pmatrix}_0 .*$$

As a consequence of the near commensurability of the frequencies ν_1 and $2\nu_2$ these upper-stage bands are widely dispersed on both sides of the fundamental frequency ν_2. This suggests the possibility that the band q_2 is a high-frequency member of this group. An examination of the energy relations of the carbon dioxide molecule or of the appropriate portion of the energy-level diagram (Fig. 1) taken from

[1] A. Adel, V. M. Slipher, and E. F. Barker, *Phys. Rev.*, **47**, 580, 1935.

[2] A. Adel and C. O. Lampland, *Ap. J.*, **87**, 198, 1938.

* A small and irregular trickle of energy appears to extend for a short distance beyond 13.5 μ. This behavior is a function of the carbon dioxide in our atmosphere. A detailed account will appear in a future paper.

the pioneer work of Martin and Barker proves that this is indeed the case.[3]

It is possible that the weak telluric band q_1, which has its center at

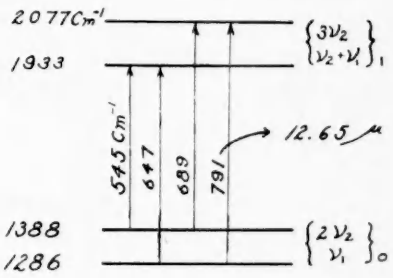

FIG. 1

approximately 11.6 μ, is similarly due to the highest frequency transition of the set

$$\begin{pmatrix} 3\nu_2 \\ \nu_2 + \nu_1 \end{pmatrix}_1 \rightarrow \begin{pmatrix} 4\nu_2 \\ 2\nu_2 + \nu_1 \\ 2\nu_1 \end{pmatrix}_0 .$$

This point is being investigated.

ARTHUR ADEL

LOWELL OBSERVATORY
FLAGSTAFF, ARIZONA
April 1, 1938

A NEW SPECTRUM VARIABLE: 5 LACERTAE

ABSTRACT

Sharp lines of H and K of *Ca* II, superposed on the broad H and K lines of the cK5 component of the composite star, 5 Lacertae (K5A0s), are found to vary in intensity and radial velocity. The velocity of the late star, regarded as constant for many years, is also found to be variable.

In the course of an examination of stars with composite spectra, the writer found that on a plate of 5 Lacertae taken in November, 1934, the H and K lines of *Ca* II were of almost interstellar sharpness and were stronger than neighboring iron lines. They were superposed on the very wide and shallow H and K lines which are characteristic of many composite spectra. Yet, on a plate taken in Octo-

[3] *Phys. Rev.*, **41**, 291, 1932.

ber, 1936, these sharp lines had completely disappeared, along with a few fainter lines in the K region, though the rest of the spectrum remained sensibly unchanged. By November, 1937, the sharp K line had definitely reappeared, together with a trace of the sharp H line and many faint lines in the wings of the broad K line.

The star 5 Lacertae (α $22^h25^m.4$; δ $47°11'$—1900; $m = 4.61$) is HD 213310–1. It has been classed as KoAo at Harvard, Mo at Mount Wilson, and K2 at Victoria. Dr. Morgan has placed it at K5 on the Yerkes system. Its trigonometric and spectroscopic parallaxes agree in assigning to it an absolute magnitude of -2 or -3.

TABLE 1

RADIAL VELOCITY IN KM/SEC

Date	K5 Star		Sharp K Line
	Vel.	Prob. Error	
Nov. 5, 1934	+21.2	± 2.1	K, +21.4 km/sec
Oct. 25, 1936	15.2	1.8	No K or H
Nov. 24, 1937	16.3	1.3	K, −20.0 } K weak; H, trace
Nov. 25, 1937	12.2	1.2	K, −10.1 }
Jan. 19, 1938	17.0	0.6	}
May 18, 1938	5.4	0.5	} Spectrum does not cover region
May 27, 1938	5.1	1.4	}
June 1, 1938	+ 5.6	± 0.7	}

In color it is redder than any normal M star. The *Henry Draper Catalogue* states: "From H to the end of shorter wave length, only the spectrum of the Ao star is visible." The star is listed as constant in light.

The star is obviously binary, though no variable radial velocity has been reported previously. The radial velocity listed in the Lick catalogue of radial velocities[1] is $-11.6 \pm .04$ km/sec. The present additional measures indicate definite variability, presumably of long range. The radial velocities, reduced to the sun, for eight plates are listed in Table 1. The plate of January 19, 1938, was taken at the Yerkes Observatory and was made available through the courtesy of Dr. Struve. The last three plates were taken, and measured, through the kindness of Dr. Petrie at Victoria, at the writer's

[1] *Pub. Lick Obs.*, 18.

request. The remaining plates were taken with the Yerkes autocollimating, one-prism spectrograph attached to the Perkins 69-inch telescope. Rapid emulsions were necessary in order to get the interesting violet region. The Victoria, Perkins, and Yerkes plates had dispersions of 15, 30, and 55 A/mm, respectively. With the exception of the Yerkes plate, there appears to be a systematic change of velocity with time, but this is not certain. The velocity variation, however, can be considered well established. Through the courtesy of Dr. Moore, the original Lick plates of 5 Lacertae were remeasured and the previous value of -11.6 was confirmed.

The sharp K line does not show the same radial velocity as the lines of the late-type star, but apparently it has a velocity variation of its own and, thus, is not interstellar but may belong to the early companion. It is most interesting that the sharp H and K lines were strongest when their radial velocities were the same as that shown by the late star, and were much fainter when their velocities differed from those of the late star. At the latter epoch the broad H and K lines of the K5 star also seemed stronger. On October 25, 1936, no sharp H and K lines appeared and the radial velocity of the late-type star was nearly the same as on November 5, 1934, at which time the sharp H and K lines and the late-type lines had the same radial velocity; hence, the secondary may be partially or totally eclipsed. However, the constancy of light seems to preclude this explanation. Artificial composite spectra made directly at the Perkins telescope have shown that in combining a Ko and an Aos star, the resulting composite K line always shows a sharp core, and it is difficult to explain the disappearance of the early K line without an eclipse, thus leading to an apparent contradiction. More observations in the near future are necessary before any definite mechanism can be assumed.

The early star is classified correctly as Aos, since the narrow H and K lines could not belong to a later type, while no B-type lines, especially *He* 1 4026, are found. The late component shows no *TiO* bands in the green, and hence the Victoria K2, or the Yerkes K5, classification can be adopted. The star is clearly a supergiant according to both its color and its parallax.

The writer hopes that the star will be placed on a photometric

program at some observatory to check for the small light variation which can be expected if the spectrum changes are the result of an eclipse.

J. A. HYNEK

PERKINS OBSERVATORY
DELAWARE, OHIO
June 15, 1938

ERUPTIVE PROMINENCES AND IONOSPHERIC DISTURBANCES

It has recently been shown[1] that every solar eruption causes a disturbance in the ionosphere, and that the intensity of the disturbance does not depend on the distance of the eruption from the center of the sun's disk.[2] The case of eruptions occurring within a few degrees of the limb is presented in the accompanying table, in which important eruptive prominences observed with a spectrohelioscope at the Commonwealth Solar Observatory, Canberra, are given, together with ionospheric effects, as determined by Mr. A. J. Higgs with the Observatory P'f equipment. The estimated central meridian distance is given for the base of the prominence.

Date	E.A.S.T.	C.M.D.	Height in Kilometers	Ionosphere Disturbances
1936 Sept. 2...	9^h15^m—10^h30^m	82°	225×10^3	F_2 disturbance 9^h15^m—9^h30^m
1937 July 3...	13 28 —13 49	90	75	No effect
26...	16 02 —16 38	>90	350	No effect
31...	10 59 —11 22	>90	120	No effect
Aug. 27...	14 08 —14 58	85	60	Fade-out 13^h10^m—13^h50^m
Sept. 15...	11 — 39	>90	225	No effect
15...	12 22 —12 44	>90	75	No effect
Oct. 13...	12 36 —13 12	85	210	Fade-out 12^h30^m—13^h10^m
25...	9 10 —11 22	90	60	Fade-out 8^h30^m—9^h35^m
Dec. 9...	15 39 —16 34	>90	235	No effect
1938 Feb. 24...	12 49 —12 53	>90	150	No effect
Mar. 16...	12 12 —13 04	>90	110	No effect

From the accompanying table it is seen that no solar eruption the base of which is behind the limb causes an ionospheric disturbance. It would seem then that *La* or other ultraviolet radiation which can

[1] *Nature*, **140**, 603, 1937. [2] *M.N.*, **97**, 605, 1937.

affect the ionosphere has its origin at the seat of the eruption, and that it is not emitted in appreciable quantities from the bright material comprising the eruptive prominence itself.

R. G. GIOVANELLI

COMMONWEALTH SOLAR OBSERVATORY
CANBERRA, AUSTRALIA
March 24, 1938

VARIABLE HYDROGEN EMISSION IN THE SPECTRUM OF γ URSAE MAJORIS

γ Ursae Majoris (Aon) shows not only *Hα* emission but a rather peculiar spectrum for a star of its class. A series of plates of the spectrum in the visual region recently taken with the Yerkes auto-collimating spectrograph attached to the 69-inch reflector of the Perkins Observatory reveal a weak emission line in the core of the broad *Hα* absorption line. The star is not listed in Merrill's "Catalogue of Be and Ae Stars."[1]

Our first plate, taken April 19, 1938, on *Hα* emulsion, showed definite but weak emission centered in the core of *Hα*. The absorption profile was unsymmetrical, being steeper on the violet side, so that the emission component appeared to lie on the violet side of the center of the line as a whole. The absorption line has extensive wings which cover an interval of about 60 A. The core appears to be about 10 A wide. On April 27 (III F plate) the emission component was much less conspicuous, and it appeared to be shifted to the violet edge of the core. Our spectrogram of May 3 showed essentially the same line structure. On the following night the emission component was even more diffuse. In fact, there was some doubt whether it actually existed. A microphotometer tracing suggested its presence by a slight hump on the violet edge of the core.

An attempt was made to secure another photograph on III F emulsion on May 23, but clouds cut it short. The spectrum was so

[1] *Ap. J.*, **78**, 87, 1933; *Mt. W. Contr.*, No. 471.

thin that little could be seen, and a microphotometer tracing showed nothing definite other than slightly greater strength in the violet half of the profile. On June 5, however, the emission core was again definitely shown. It appeared as strong as it had on our first plate and considerably stronger than it had on any of the later plates. This time it again appeared centered on the absorption core, but slightly to the red of the center of the line as a whole. Our plate of June 9 showed no emission component at *Hα*.

The rest of the spectrum was investigated. A preliminary glance showed nothing but the two hydrogen lines, but a careful examination revealed a number of very wide and extremely shallow absorption lines. They were from 10 to 15 A wide and were so shallow as to be almost invisible through lack of contrast. Sixteen lines were definitely located, and several other fainter ones are probably present. Although only the roughest measurement was possible, the lines were identified with those of ionized metallic atoms. The consistency of the correspondence between these shallow absorption lines and the strongest emission lines in the spectrum of γ Cassiopeiae lends plausibility to the identifications. The accompanying list was found. The last line was much sharper and darker than the

λ 4924	*Fe* II	λ 5535	*Fe* II
5018	*Fe* II	5890	*Na* I
5056	*Si* II	5896	*Na* I
5169	*Fe* II	5979	*Si* II
5184	*Ti* II	6347	*Si* II
5198	*Fe* II	6371	*Si* II
5226	*Ti* II	6456	*Fe* II
5317	*Fe* II	6516	*Fe* II

others. The *Na* D lines were extremely diffuse. Some of these lines were recorded by Miss Waterman.[2]

On the plates of June 5 and 9 a weak emission component appeared in the core of *Hβ*. Owing to curvature of field in the grating spectrograph the focus is never sharp at *Hβ*. Consequently I do

[2] *Lick Obs. Bull.*, **8**, 1, 1913.

not attach much weight to the appearance of that line on any plate. I merely mention this observation for the interest of others who may care to follow the star with a prism spectrograph.

ERNEST CHERRINGTON, JR.

PERKINS OBSERVATORY
DELAWARE, OHIO
June 9, 1938

REMARKS ON THE PAPER "THE SODIUM CONTENT OF THE HEAD OF THE GREAT DAYLIGHT COMET SKJELLERUP 1927 K"

In Section IV of this paper we have estimated the magnitude of the cometary head in the light of the D lines, combining the approximate dimensions of the comet's atmosphere with the density of the normal sodium as determined in Section III. In doing so we assumed the monochromatic magnitude to be proportional to the mean density. But according to the foregoing considerations in our paper, especially Figure 4, page 356, this assumption is only fulfilled up to $C \sim 0.2$ or $Nf \sim 3.3$, where N is the number of normal atoms per cubic centimeter and f the line strength. Putting $f = 1$ and $N = 3.3$ for the sum of both D lines, and using the values given on pages 357–358 of our paper, one gets for the ratio of the sun's apparent brightness and that of comet Skjellerup's head $F = 3.5 \times 10^{11}$.

Our Figure 4 quoted above shows further that the intensity of the D lines increases 4.5-fold if N increases from 3.3 to 50—that is, to its lower limit calculated in Section III. With $N = 50$ one gets

$$F = \frac{3.5 \times 10^{11}}{4.5} = 7.8 \times 10^{10},$$

and putting this equal to 2.5^x, $x = 27.4$; therefore the temporary monochromatic magnitude of the comet's head was

$$M = 27.4 - 26.7 = +0.7,$$

a value which is compatible with the subjective estimate of Mr. Slipher mentioned in Section I.

The upper limit of the sodium density found in Section III, $N = 2500$ ($C = 150$), would give approximately the same intensity of the D lines (see Fig. 4)—so that under the peculiar conditions of the comet the estimated monochromatic magnitude of the comet's head does not allow us to decide between the upper and the lower limits of the amount of sodium calculated in Section III.

ARTHUR ADEL
V. M. SLIPHER
R. LADENBURG

LOWELL OBSERVATORY, FLAGSTAFF, ARIZONA
PALMER PHYSICAL LABORATORY, PRINCETON UNIVERSITY
June 1938

ERRATUM

Dr. T. E. Sterne calls attention to a misprint on page 149, section 5, line 19, of his article, "The Secondary Variation of Delta Scuti," in the March, 1938, issue of the *Astrophysical Journal* (Vol. **87**). The word "possible" should read "impossible."